Association Euratom - Risø National Laboratory annual progress report 2004

Bindslev, H.; Singh, B.N

Publication date:
2005

Document Version
Publisher's PDF, also known as Version of record

Risø-R-1520(EN)

Association Euratom - Risø National Laboratory Annual Progress Report 2004

Edited by H. Bindslev and B.N. Singh

Risø National Laboratory, Roskilde, Denmark
June 2005

Abstract The programme of the Research Unit of the Fusion Association Euratom - Risø National Laboratory covers work in fusion plasma physics and in fusion technology. The fusion plasma physics research focuses on turbulence and transport, and its interaction with the plasma equilibrium and particles. The effort includes both first principles based modelling, and experimental observations of turbulence and of fast ion dynamics by collective Thomson scattering. The activities in technology cover investigations of radiation damage of fusion reactor materials. These activities contribute to the Next Step, the Long-term and the Underlying Fusion Technology programme. A summary is presented of the results obtained in the Research Unit during 2004.

ISBN 87-550-3449-7
ISSN 0106-2840; 1396-3449

Foreword

Risø participates in the internationally coordinated activities to develop fusion as a major source of energy. The principle being pursued is the fusion of hydrogen isotopes to form helium. This is the process, which powers the sun. To make the fusion process run at a significant rate the hydrogen gas must be heated to high temperatures where it ionises and turns into a plasma. Furthermore, the plasma must be confined to achieve suitable densities and sustain the high temperature. On the sun gravity provides the confinement. On earth, the line we are pursuing, use a magnetic field for the confinement. While fusion holds the promise of providing a sustainable source of energy, which is environmentally sound, it also presents considerable scientific and engineering challenges. Key issues in the final steps towards realising fusion energy production include:

1. Improving the plasma energy confinement, that is the ratio between the energy of the plasma and the heating power required to sustain the plasma energy. Improving energy confinement implies reducing energy transport out of the plasma, which principally is due to turbulence. So what we really need to do is to understand and control turbulence.
2. Channelling the energy of fast ions, produced in fusion reactions, into heating the bulk plasma without driving turbulence and without premature exit of the fast ions from the plasma. This requires understanding and control of the dynamics of the fast ions in interaction with other particles and with waves.
3. Development of materials, which maintain required mechanical properties under high and sustained neutron fluxes. Neutrons, produced in the fusion reactions, are not confined by the magnetic field. They pass through the first wall of the chamber surrounding the plasma, slowing down on impact with atoms in the wall, thereby giving rise to dislocations in the wall material, which affect the properties of the material.

Risø contributes to fusion research in all these areas: 1) codes, modelling turbulence and transport, have been developed and are continually improved, and benchmarked against experiments. 2) Central to understanding the dynamics of fast ions is the acquisition of temporally and spatially resolved measurements of the fast ion velocity distributions in the plasma. Risø, in collaboration with MIT (USA) and EURATOM partners, is developing millimetre wave based collective Thomson scattering (CTS) diagnostics at the TEXTOR and ASDEX upgrade tokamaks in FZ-Jülich and the Max-Planck Institute for plasma physics in Garching (near Munich). Of particular note this year has been EURATOM-Risø's investigation of the feasibility of measuring fast ion dynamics in the next step fusion device, ITER, by CTS. This study, encompassing essentially all potential CTS probe frequencies, found that a millimetre wave system was the best option, that such a system could meet all the measurement requirements set out by the ITER team and it could be built with present or near term technology. 3) In the field of irradiated materials research Risø is investigating the properties of copper alloys relevant to the next step in fusion research, ITER, and of iron alloys, which will be an essential component of a commercial fusion power plant.

Henrik Bindslev
Risø National Laboratory
April 2005

Contents

1. Summary of Research Unit activities

The activities in the Research Unit cover two main areas:

Fusion Plasma Physics, which includes:

- *Theoretical and numerical turbulence studies*. Turbulence and the associated anomalous transport is investigated using first principles based models and solving these by means of numerical codes in full toroidal geometry. These models are continuously being developed and benchmarked against existing codes at other associations. The dynamics of bursts of fluctuations leading to profile relaxation have been studied in models for flux-driven interchange mode turbulence, where the back reaction of the turbulence on the equilibrium flows and profiles are accounted for.
- *Fast Ion Collective Thomson Scattering.* Risø has taken the lead in the development of fast ion collective Thomson scattering diagnostics for TEXTOR, ASDEX upgrade (AUG) and ITER. These projects are carried out in close collaborations with MIT, and with the TEC[†] and AUG teams.

Fusion Technology, which includes:

- Experimental and theoretical investigations of the effects of irradiation on the microstructural evolution and on the physical and mechanical properties of metals and alloys relevant to the Next Step, the Long Term and Underlying Fusion Technology Programme.

The **global indicators** for the Research Unit in 2004 are:

• Professional staff	13.9	man-years
• Support staff	7.5	man-years
• Total expenditure - incl. mobility	3.01	MioEuro
• Total Euratom support	0.77	MioEuro

[†] TEC: the Trilateral Euregio Cluster, a collaboration of FOM Institute for Plasma Physics, Holland; ERM/KMS, Belgium and Forschungszentrum Jülich, Germany.

2. Plasma Physics and Technology

2.1 Introduction

H. Bindslev
henrik.bindslev@risoe.dk

At the start of 2004, the research programme changed name from *Plasma and Fluid Dynamics* to *Plasma Physics and Technology*. As a follow-on from that, the department changed name to *Optics and Plasma Research Department.* This change of name reflects our commitment to concentrate and build on our core competence in plasma physics, spanning the field from the high temperature plasmas required for fusion energy to low temperature plasmas for a broad range of current and near-term environmental and industrial applications. The latter include cleaning of exhaust gases, sterilisation, material synthesis, and modification of surfaces for instance to improve adhesion.

A plasma is a dense collection of free ions and electrons. The transitions from solids to fluids to gases are associated with increases in internal energy, the breaking of bonds and changes of physical properties. The same is true of the transition from a gas to a plasma; in fact the plasma is rightfully described as the fourth state of matter, its physics differing as much from that of gases as that of solids does. Just as solid state physics is involved in a broad range of applications, so it should be no surprise that plasmas have a wide range of applications, that their physics and chemistries are rich, and that the methods of generation and diagnosis are wide and complex.

Our activities in high temperature plasmas, aimed at developing fusion energy, are coordinated with the European EURATOM fusion programme through an agreement of association on equal footing with other fusion laboratories in Europe. Our EURATOM association facilitates extensive collaboration with other fusion research laboratories in Europe, crucial in the ongoing build-up of competencies at Risø, and gives us access to placing our experimental equipment on large fusion facilities at the Max-Planck Institute for Plasma Physics in Garching and at the Research Centre Jülich, both in Germany. Our association with EURATOM also provides the basis for our participation in the exploitation of the European fusion research centre, JET, located in England. With its organisation of national programmes as EURATOM associations, the European fusion programme is a successful example of a large *European Research Area.* Our activities in high temperature plasma research and the development of fusion energy are introduced in subsection 2.1.1, and described in further detail in subsection 2.2 discussing turbulence and transport in fusion plasmas, and in subsection 2.3 discussing our use of millimetre waves for investigating the dynamics of fast ions in fusion plasmas.

2.1.1 Fusion plasma physics

H. Bindslev
henrik.bindslev@risoe.dk
www.risoe.dk/euratom

Producing significant amounts of fusion energy requires a plasma with a temperature of 100 to 200 million degrees and densities of 1 to 2 times 10^{20} particles per cubic metre, corresponding to a pressure of 1 to 5 atmosphere. Unlike gases, plasmas can be confined and compressed by magnetic fields. At the required temperatures the plasma must be lifted off material walls to prevent the plasma from rapid cooling. This is done by suspending the plasma in a toroidally shaped magnetic field that also acts to balance the plasma pressure. The required temperature and densities have been achieved in the joint European fusion experiment, JET. The production of net energy adds the requirement that the energy in the plasma be confined at least on the order of six seconds. The confinement time is the characteristic time for cooling off if heating was switched off or, equivalently, the ratio of plasma energy to required heating power to sustain that energy content. Achieved confinement times are on the order of one second. Higher density could compensate shorter confinement time and visa versa, so a simplified statement of the target is that the product of temperature, density and confinement time should be six atmosphere × seconds and is currently one atmosphere × seconds. Progress towards the goal principally involves improving the confinement time or, equivalently, reducing the energy transport in the plasma. The energy transport in fusion grade plasmas is principally due to turbulence, one of our main research activities reported in subsection 2.2. Significant progress towards the goal is expected with the next step fusion experiment, ITER, which has been designed and is currently being negotiated between the participants, i.e. Europe, Japan, Russia, USA, China and Korea. In ITER significant fusion rates are expected and with that the fast ion populations in the plasma will increase dramatically compared with present machines. The fast ions may then influence the plasma significantly. As a consequence, the dynamics of fast ions and their interaction with the rest of the plasma is one of the central physics issues to be studied in ITER. It is in fact also one of our main research topics in fusion as reported in subsection 2.3.

The fields of turbulence, transport and fast ions are closely knit. With steep gradients in plasma equilibrium parameters and with populations of energetic ions far from thermal equilibrium, fusion plasmas have considerable free energy. This energy drives turbulence, which in turn acts back on the equilibrium profiles and on the dynamics of the fast ions. The turbulence naturally gives rise to enhanced transport, but also sets up zonal flows that tear the turbulent structures apart and result in edge transport barriers; most likely at the root of the poorly understood, but experimentally reliably achieved, high confinement mode (H-mode). This non-linear interplay between turbulence and equilibrium also supports transient events reminiscent of edge localised modes (ELMs) where energy and particles are ejected from the plasma edge in intermittent bursts.

This set of topics is the focus of our fusion plasma physics research: With first-principles based codes we seek to model the interplay between plasma turbulence, transport and equilibrium. This modelling is tested against experimental data in collaboration with other fusion plasma physics institutes. To elucidate the physics of fast ions and their interplay with turbulence, waves and transient events, we are engaged in the diagnosis of confined fast ions by collective Thomson scattering (CTS) at the TEXTOR tokamak at the Research Centre Jülich and at the ASDEX upgrade tokamak in the Max-Planck Institute for Plasma Physics in Garching, both in Germany.

Our aim is not only to understand the dynamics, but also to identify external actuators with which the turbulence and transport can be controlled. The first demonstrations of edge turbulence control with arrays of electrostatic probes have been made in a linear device in collaboration with other associations. Selective ejection of core fast ions by sawteeth, which in turn can be manipulated by a localised heating and current drive, was found in fast ion CTS data obtained at TEXTOR in collaboration with TEC[1] and MIT, USA.

1. TEC: the Trilateral Euregio Cluster, comprising Association EURATOM-Forschungszentrum Jülich GmbH, Institut für Plasmaphysik, Jülich, Germany; Association EURATOM-FOM, Institute for Plasma Physics, Rijnhuizen, Netherlands; and Association EURATOM-ERM/KMS, Belgium.

2.2 Turbulence and transport in fusion plasmas

O. E. Garcia, V. Naulin, A. H. Nielsen and J. Juul Rasmussen
volker.naulin@risoe.dk; jens.juul.rasmussen@risoe.dk

The transport of heat and particles across the confining magnetic field of fusion plasmas is one of the most important and interesting, but also most difficult areas of contemporary fusion research. It is well established that the "anomalous" transport component mediated by low frequency turbulence is far larger than the classical collisional transport. It is thus of utmost importance to achieve a detailed understanding of this transport and the underlying turbulence for the design of an economically viable fusion reactor based on magnetic confinement schemes. In spite of dramatic progress in experiment, theory and computations during recent years, the quantitative understanding is still very sparse and any predictive capacity is at best rudimentary. Even very fundamental phenomena such as transitions from low confinement regime (L-mode) to high confinement regime (H-mode), the profile resilience and the particle pinch that are routinely observed and classified experimentally have no generally accepted explanations.

We have mainly focussed our activities in plasma turbulence and transport on topics related to edge turbulence. It is found that the conditions near the edge of the plasma are dictating the global performance, which seems natural since all transport has to go through the edge region. Our investigations are based on numerical solutions of first-principle models, and we aim at benchmarking results and performance with other codes and also with experimental observations when available.

Our investigations have comprised direct numerical simulations of the transport of impurities in the edge plasma region (see subsection 2.2.1), where we found strong asymmetric transport features with dominating pinch convection on the low-field side and an anti-pinch, i.e. outward convection, at the high-field side. We have furthermore investigated the influence of finite inertia effects on the mixing and transport of impurities (see subsection 2.2.2), where we observed a local clustering of the impurity density in vortical structures and an additional pinch effect; both of these features were found to scale with the mass to charge ratio of the impurities. The up-gradient transport and the profile resilience were examined by using a probabilistic transport model with two different particle step lengths depending on the local value of the gradient (see subsection 2.2.3). This serves as a phenomenological model for the interplay between classical transport and anomalous transport setting in when the gradient exceeds a critical value. Indeed profile peaking and resilience could be obtained for off-axis fuelling.

In subsections 2.2.4, 2.2.5 and 2.2.6 we consider the bursting and intermittency in the fluxes of particles and heat in the edge and scrape-off-layer (SOL) of a toroidal plasma. The

key mechanism here is the nonlinear energy exchange between global poloidal flows and small-scale turbulent fluctuations. In subsections 2.2.4 and 2.2.5 we have employed the energy conserving global model for interchange dynamics at the transition from the edge to the SOL. Results from this model are directly compared with recent experimental observations and reproduce in detail the observations of plasma blobs propagating far out into the SOL (see subsection 2.2.4). These propagating blobs are responsible for strongly intermittent bursts of hot plasma, which pose a serious problem to plasma facing components in next generation devices like ITER. Comparison of the statistical properties of ion and electron energy fluxes to the divertor plates is envisaged as a next step.

The self-consistent generation of large-scale flows by rectification of the small-scale turbulent fluctuations is receiving increasing interest in recent years. These flows can set up transport barriers and are assumed to play a crucial role in the transition from the low confinement to the high confinement regime (LH-transition) and also for internal transport barriers. However, the exact mechanisms for flow generation have not been quantitatively assessed yet. We have investigated the generic flow generation from turbulence in drift-Alfvén turbulence in subsection 2.2.7. By covering a broad range of parameters we have revealed the relative importance of the different sources and sinks for the flows. The Reynolds stress is always acting as a source for the flow, but for increasing plasma beta the so-called Maxwell stress, which is due to magnetic field fluctuation, comes into play. This is a sink for the flow energy and eventually counteracts the Reynolds stress limiting flow generation. However, a third effect arising from the geodesic part of the magnetic field curvature and being a sink for low beta values changes sign for higher beta values and in this regime becomes the main drive for the flows. These results indicate that it may be misleading to project the strength of large-scale flow mediated transport barriers from low beta plasmas to high beta plasmas in, e.g., ITER.

Finally, in subsection 2.2.8, we show the results of a linear analysis of the drift-wave mode structure in a collisional plasma. Predictions from linear theory taking proper account of the spatial dependence of collisionality are in detailed agreement with experimental observations, paving the way for a detailed comparison between turbulent experimental states and fully non-local 3D simulations.

2.2.1 Impurities in tokamak edge turbulence

V. Naulin
volker.naulin@risoe.dk

Transport of impurities through the edge region of a toroidal confinement device is still poorly understood. Modelling of experimental results shows that we have to invoke anomalous effects to explain the observed impurity concentrations. These effects include anomalous diffusion coefficients as well as anomalous pinch velocities. We here investigate the transport of ideal, in the sense of massless, passive particles under the action of electromagnetic drift Alfvén turbulence.

We recover the curvature-related particle pinch for the impurities, which is predicted within the concept of turbulent equipartition. The net inward pinch velocity of the impurities then results from a combination of the curvature pinch (which is inward on the low-field side and outward on the high-field side) with the ballooning properties of the turbulence.

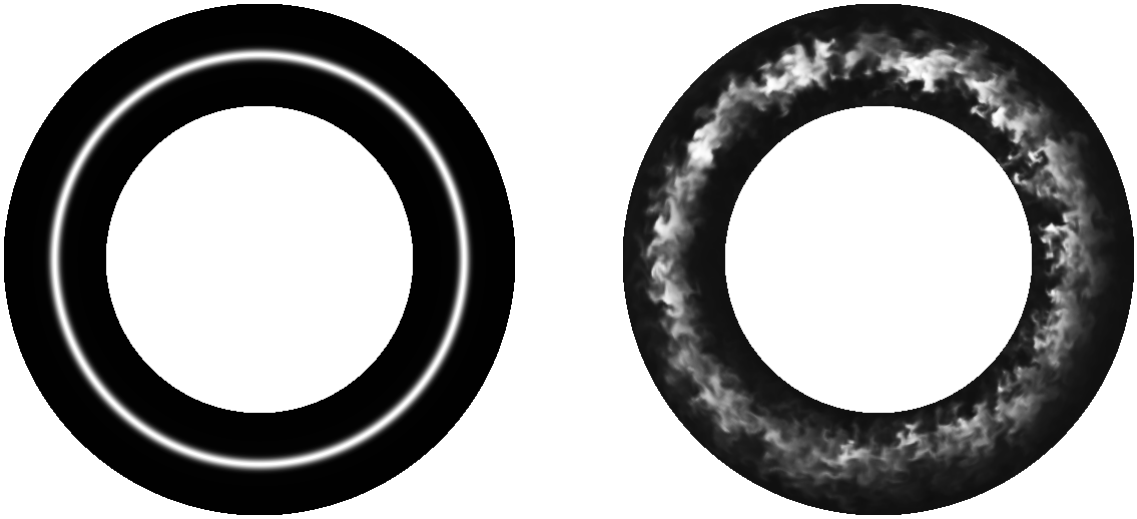

Figure 1. Poloidal cross section showing initial impurity density and impurity density after some turbulent mixing.

Using turbulent equipartition, an approximate relationship between anomalous diffusion and anomalous pinch can be found, a relationship that is confirmed by the numerical simulations.

1. V. Naulin, Impurity and trace tritium transport in tokamak edge turbulence, Physical Review E **71**, 015402, (2005).

2.2.2 Anomalous diffusion, clustering and pinch of impurities in plasma edge turbulence

M. Priego, O. E. Garcia, V. Naulin and J. Juul Rasmussen
jens.juul.rasmussen@risoe.dk

It is well established that turbulence is the dominant transport mechanism for particles and heat in the edge region of magnetised plasmas. Turbulence moreover has a strong influence on the transport of impurities in this region. Pinching of impurities, i.e. a fast convective inward transport, is generally observed in experimental investigations in addition to the turbulent diffusive spreading. This has also been the case for the trace-tritium transport investigations in JET.[1]

We have investigated the turbulent transport of impurities in plasma edge turbulence employing the two-dimensional Hasegawa-Wakatani model for resistive drift-wave turbulence. The impurity evolution is modelled by tracing a passive scalar field in the self-consistently developed turbulence obtained from the solution of the Hasegawa-Wakatani equations. Various features of the impurity transport are examined by means of numerical simulations using a novel code that applies semi-Lagrangian pseudo-spectral schemes. In particular, we have investigated the influence of finite inertia in the advection of the impurities. This influence is accounted for in the polarisation drift and is becoming increasingly important for rising mass-charge ratio of the impurity species. In this case the velocity field experienced by the impurity field is compressible, which will lead to local accumulations of the impurities and which will also be instrumental in the pinch effect. Correspondingly we found that the density granulation of the impurities is correlated with the vorticity field, i.e. impurities cluster in vortices of positive vorticity, while they are expelled from vortices of negative vorticity as illustrated in Figure 2. In addition, we observed a radial

pinching of the impurities. Both the clustering effect and the pinching are increasing with rising mass-charge ratio of the impurities.

1. K.D. Zastrow, Nucl. Fusion **39**, 1891 (1999).

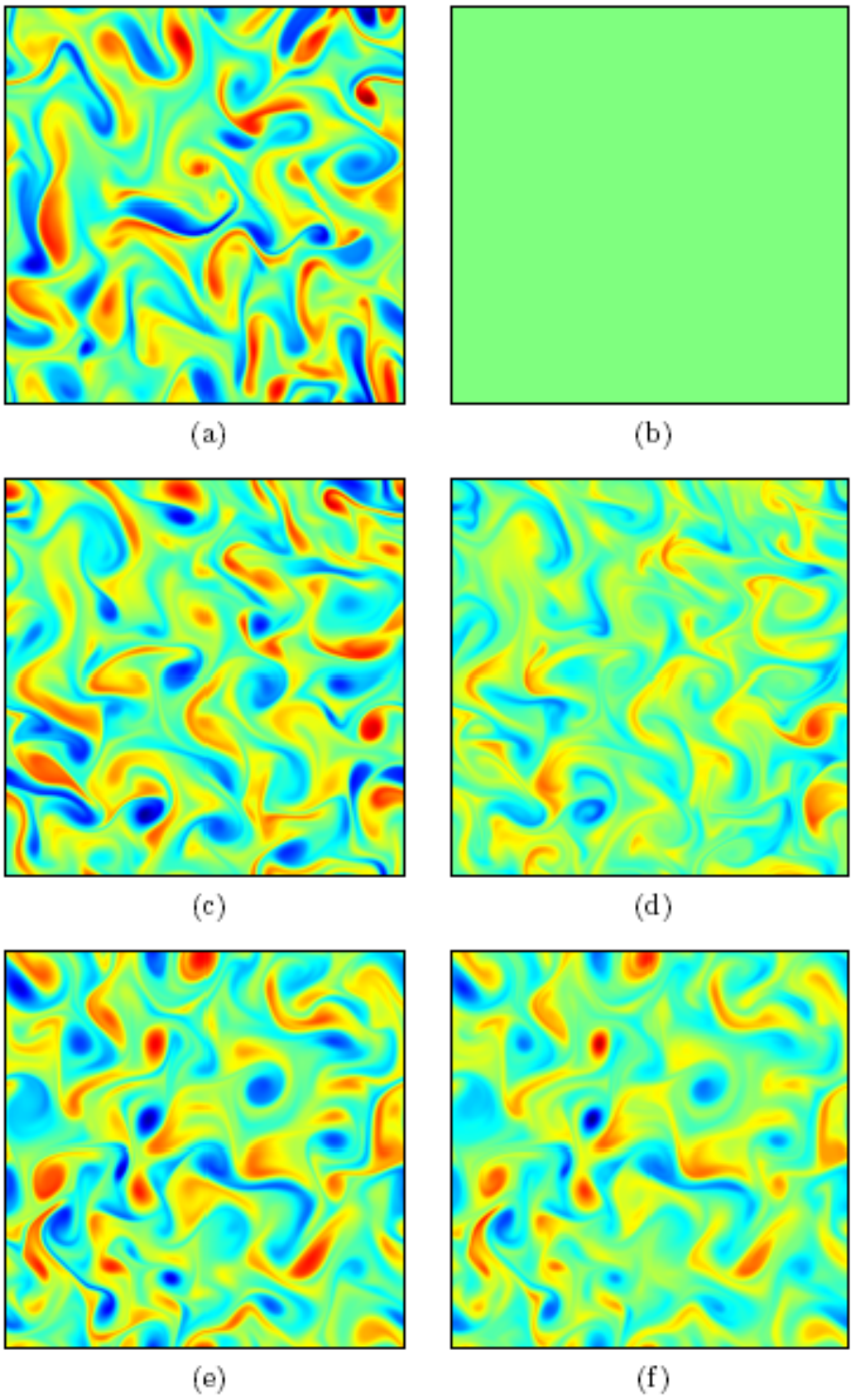

Figure 2. Fig. 1. Time evolution of the vorticity field (left panel) and the perturbation of an initially (t = 0) uniformly distributed impurity density (right panel). (a,b) t = 0, (c,d) t = 5 and (e,f) t = 50. Blue represents negative values and red represents positive values.

2.2.3 On the up-gradient transport in a two-step diffusion model

O. E. Garcia, J. Gavnholt, V. Naulin, A.H. Nielsen and J. Juul Rasmussen
jens.juul.rasmussen@risoe.dk

The cross-field transport of particles and heat in magnetically confined hot plasmas is a complex and only partially understood issue. It is composed of several elements including classical and neo-classical collisional diffusion and anomalous turbulent transport. Several "strange" features characterise the transport. Examples are up-gradient transport (i.e. transport in the direction of the gradient), profile resilience or consistency (i.e. the existence of stiff profiles that are only weakly dependent of the fuelling), rapid transport phenomena (i.e. perturbative transport events that are significantly faster than the diffusive transport derived from the background gradients). These features cannot consistently be explained by simple "Fickian" diffusion in which the transport is assumed to be governed by diffusivities.

Recently, van Milligen *et al.*[1] have proposed a probabilistic model for the description of the transport and the evolution of the density profile in a plasma with external sources. The model is based on an explicit time- and space-dependent particle step probability distribution function, PDF. This PDF is assumed to depend on the local density gradient. When the gradient is below a critical value, the PDF is a Gaussian distribution with a standard deviation ("step size") σ_2; this will correspond to a normal diffusive process and mimics the collisional diffusion. However, when the gradient is larger than a critical value, the PDF is argued to be of the Lévy type, i.e. with no characteristic length scale. This shall mimic the anomalous transport mediated by turbulence and shall signal that there are long-range correlations. Van Milligen *et al.*[1] have solved this model for many different situations with various source distributions and have found that it reproduces several of the "strange" features mentioned above. It was strongly emphasised that the Lévy-type particle step PDF is essential for the observed characteristics.

We have re-examined the model of van Milligen *et al.* to investigate the sensitivity of the results on the assumed particle step PDFs. In particular, we have solved the model for the case where also the PDF for supercritical gradients is a Gaussian with a "step size" $\sigma_1 > \sigma_2$. We have basically reproduced the transport features observed by van Milligen *et al.* In Figure 3 we show the typical density profile when the fuelling is off-axis for the case of two Gaussian particle step PDFs, with $\sigma_1 = 0.08$ and $\sigma_2 = 0.02$. The density profile is clearly peaked in the centre and is very similar to the profile obtained for the case when the particle step PDF for supercritical gradients is a Cauchy (Lévy) distribution as used in ref. 1. We should note that we obtained a similar profile using asymmetric off-axis fuelling, i.e. only one source displaced from the centre. In Figure 4 we demonstrate the profile consistency by plotting the central density, $n(x = 0.5)$, for different source strengths, S_0 and various particle step PDFs. It is observed that $n(x = 0.5)$ is roughly constant over a broad range of source strengths S_0, for the case of a Gaussian and Cauchy PDF as well as for two Gaussians when $\sigma_1 > 2\text{-}3\ \sigma_2$. This is a signature of profile consistency. We have thus demonstrated that the essential feature for obtaining profile peaking and consistency in transport models is the existence of a step size PDF regulated by a critical gradient. The effective step size above the critical gradient, in the anomalous channel, must be sufficiently larger than the step size in the classical channel. However, it is not necessary to have a Lévy type PDF for the anomalous transport channel.

1. B.Ph. van Milligen, B.A. Carreras, and R. Sánchez, Phys. Plasmas **11**, 3787 (2004); ibid **11**, 2272 (2004).

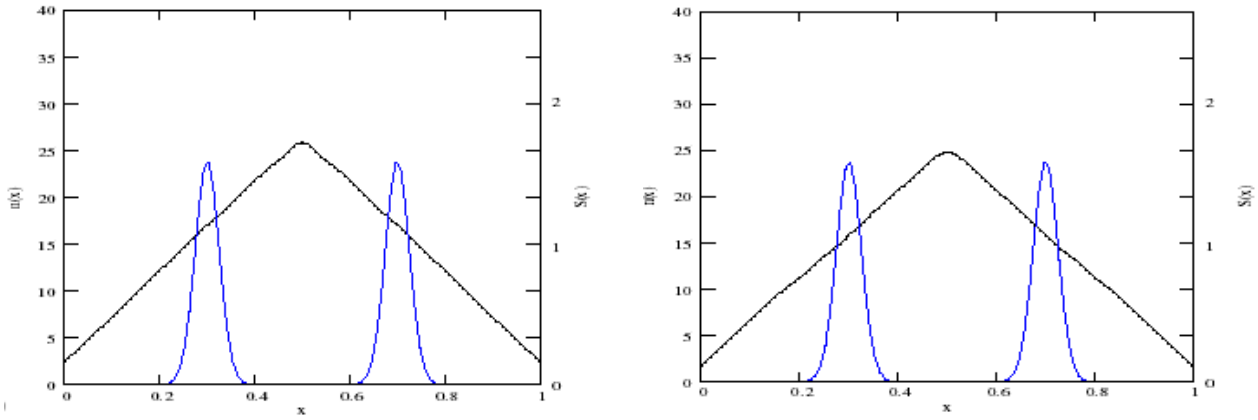

Figure 3. The density profile with symmetric off-axis fuelling. The sources are shown by the blue curves ($S_0 = 0.2$), for different transport step size PDFs. (a) Two Gaussian distributions with the step sizes: $\sigma_1 = 0.08$ and $\sigma_2 = 0.02$. (b) A Cauchy and a Gaussian distribution as used by van Milligen et al.[1]

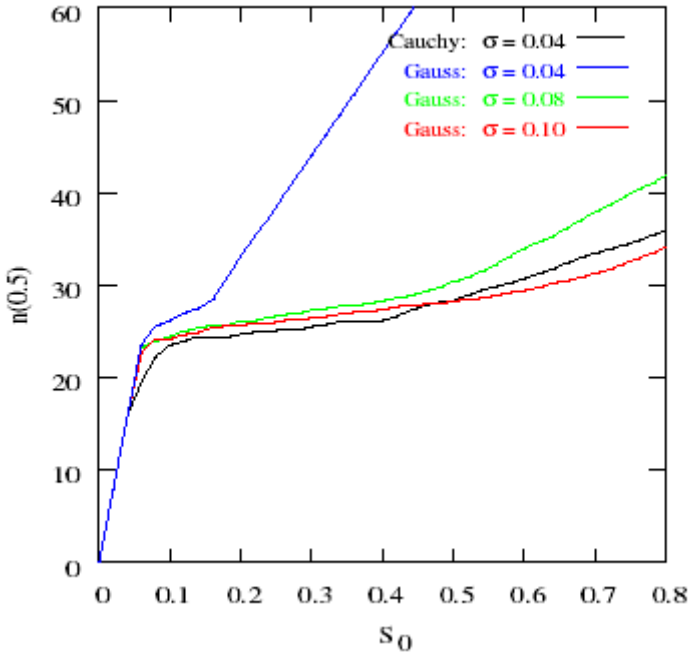

Figure 4. Profile "stiffness" shown by the dependence of the central density on the source strength S_0, for the cases where the anomalous transport channel is characterised by a Cauchy distribution and the cases where it is a Gaussian with the values of σ_1 shown in the caption.

2.2.4 Simulations of blob propagation in edge and scrape-off layer of toroidal plasmas

A. H. Nielsen, O. E. Garcia, O. Grulke (MPI for Plasma Physics, EURATOM Association, Greifswald, Germany), V. Naulin and J. Juul Rasmussen
anders.h.nielsen@risoe.dk

Numerical fluid simulations of interchange turbulence for geometry and parameters relevant for the boundary layer of magnetic confinement devices have shown to result in intermittent transport qualitatively similar to many recent experimental measurements. The two-dimensional simulation domain features a forcing region with spatially localised sources of particle and heat outside which losses due to motion along open magnetic field lines

dominate, corresponding to the edge and the scrape-off layer (SOL), respectively.[1,2] The results obtained from the simulations are compared with experimental observations at the Alcator C-Mod.

In turbulent states we observe intermittent eruptions of hot plasma from the edge region, propagating radially far into the SOL in the form of field-aligned filaments, or blobs. Here they are dissipated due to transport along open magnetic field lines. In between these quasi-periodic bursts, the flow settles into a self-generated shear flow stopping the radial transport almost completely. The radial propagation velocity of the blobs may reach one tenth of the sound speed, in excellent agreement with experimental measurements at Alcator C-mod.

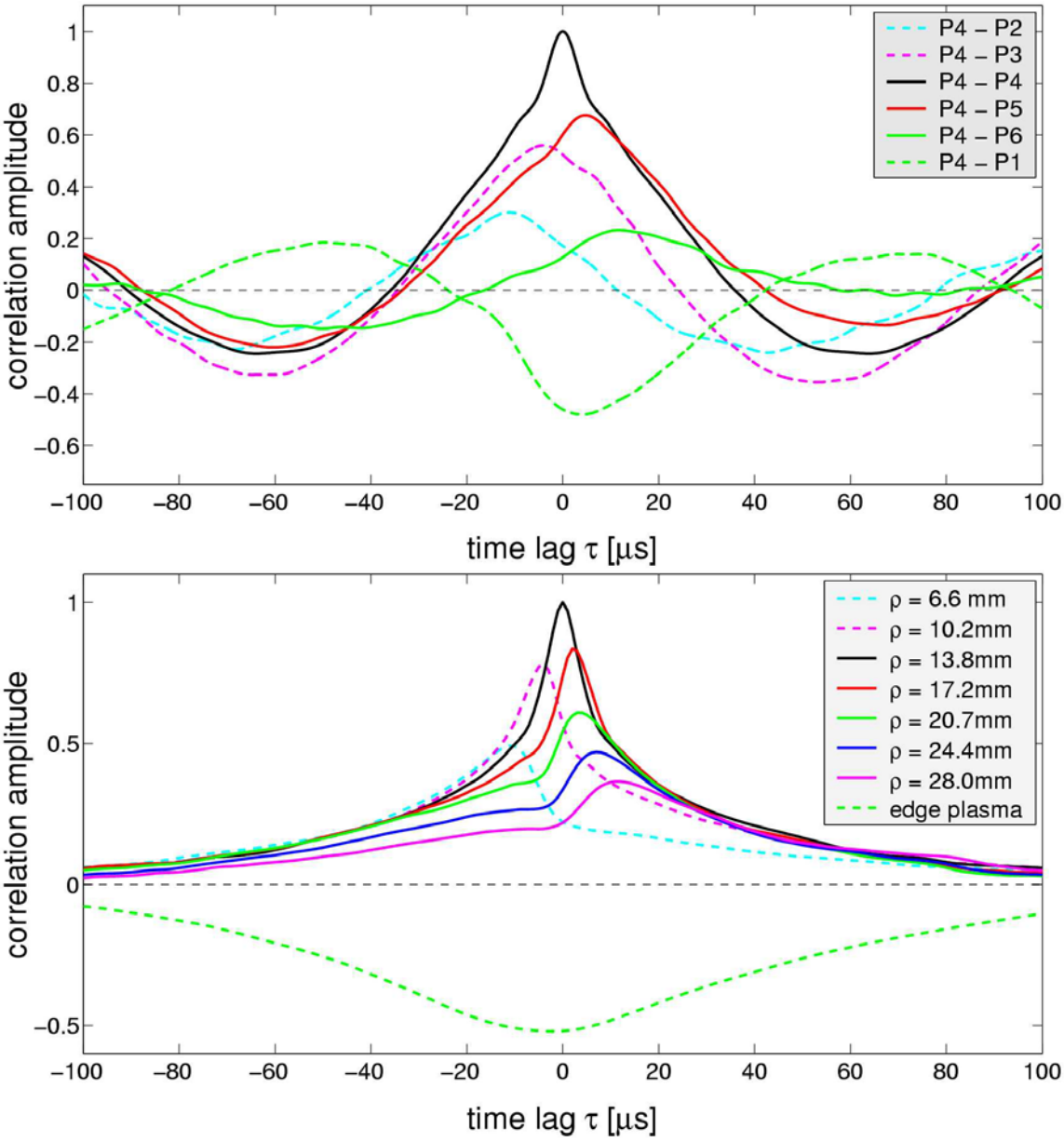

Figure 5. Top: The correlation of the density signal between P4 with the other probes. The seven probes are distributed equidistantly in the radial direction with P1 being located in the edge region and P2 at the LCFS. Bottom: the corresponding curves for the Alcator experiment.

The statistics of single-point recordings obtained at different radial positions, Pi, from the simulations have been compared with data from Alcator C-mod. An example of this

comparison is shown in Figure 5. The two frames display the correlation of the density signal between a probe located well into the SOL, P4 in the simulation, with the signal from the other probes. In both cases we observed a clear indication of an outward moving structure and we observe an anti-correlation at time = 0 for the probe located in the edge region.

1. O.E. Garcia, V. Naulin, A.H. Nielsen and J. Juul Rasmussen, "Computations of Intermittent Transport in Scrape-Off Layer Plasmas", Phys. Rev. Lett. **92**, 16 (2004).
2. O.E. Garcia, V. Naulin, A.H. Nielsen and J. Juul Rasmussen, "Turbulence and intermittent transport at the boundary of magnetized plasmas", submitted to Phys. Plasmas (2005).

2.2.5 Turbulence and intermittent transport at the boundary of magnetised plasmas

O. E. Garcia, V. Naulin, A. H. Nielsen and J. Juul Rasmussen
odd.erik.garcia@risoe.dk

A three-field fluid model for plasma density, electron temperature and fluid vorticity has been derived in order to describe the edge and scrape-off layer region of a magnetised plasma.[1,2] The model is based on interchange modes due to a non-uniform magnetic field, neglecting small-scale drift wave dynamics as well as magnetic shear. However, the fully non-linear flow compression terms are maintained in order to describe the order unity perturbation of the dependent variables that is observed experimentally.

Numerical simulations for geometry and parameters relevant to the boundary region of magnetic confinement devices are shown to result in intermittent transport qualitatively similar to many recent experimental measurements. The two-dimensional simulation domain features a forcing region with spatially localised sources of particles and heat outside which losses due to motion along open magnetic field lines dominate, corresponding to the edge region and the scrape-off layer, respectively.

In turbulent states we observe intermittent eruptions of hot plasma from the edge region, propagating radially far into the scrape-off layer in the form of field-aligned filaments, or blobs. This results in positively skewed and flattened single-point probability distribution functions of particle density and temperature, reflecting the frequent appearance of large positive fluctuations (Figure 6a). Moreover, the conditional fluctuation waveforms and transport statistics are in good agreement with those derived from experimental measurements (Figure 6b).

Associated with the turbulence bursts are relaxation oscillations in the particle and heat confinement as well as the kinetic energy of the poloidal flows. The formation of blob structures is thus related to profile variations that may be triggered in a quasi-periodic manner by a global dynamical regulation due to sheared flows. These results support the idea that any turbulence propagating into the region of open magnetic field lines leads to radial propagation in the form of blobs, thereby extending the present results to the propagation of edge localised modes.

1. O. E. Garcia, V. Naulin, A. H. Nielsen, and J. Juul Rasmussen, Phys. Rev. Lett. **92**, (2004).
2. O. E. Garcia, V. Naulin, A. H. Nielsen, and J. Juul Rasmussen, "Turbulence and intermittent transport at the boundary of magnetized plasmas", submitted to Physics of Plasmas 2005.

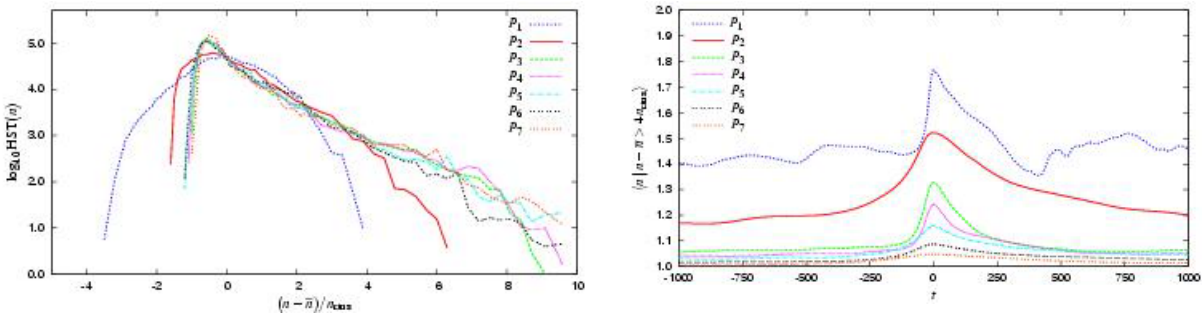

Figure 6. a) Single-point probability distribution functions of the particle density, reflecting the frequent appearance of large positive fluctuations. b) Conditional fluctuation waveforms of the density.

2.2.6 Two-dimensional thermal convection in fluids and magnetised plasmas

O. E. Garcia, V. Naulin, A. H. Nielsen, J. Juul Rasmussen and N. H. Bian
(Department of Physics, The University of Manchester, United Kingdom)
odd.erik.garcia@risoe.dk

A paradigmatic two-field fluid model describing convective motions in fluids as well as magnetised plasmas has been investigated analytically and numerically. In the fluid case, the baroclinic generation of vorticity is the source of convection, while magnetic guiding centre drifts in non-uniformly magnetised plasmas act to drive similar motions known as interchange, resistive-g and ballooning modes.[1-3]

The close relationship between these mechanisms for vorticity generation is exploited to give a new perspective for the onset of convective motions and sheared poloidal flows in magnetised plasmas. This also contradicts the general view of turbulent transport as essentially "collisionless".

Non-linear numerical simulations saturating in stationary convective states reveal the process of laminar scalar gradient expulsion, leading to the formation plumes in the pressure field as well as vorticity sheets. These dissipative structures have been demonstrated to result in temperature profile consistency and transport scaling at large Rayleigh numbers.[2,3]

In the case of self-sustained sheared azimuthal flows, the turbulence has a bursty nature associated with relaxation oscillations in the kinetic energy of the mean azimuthal flows. This leads to a state of large-scale intermittency manifested by exponential tails in the single-point probability distribution functions of the dependent variables. The global bursting may be interpreted in terms of a predator-prey regulation from the point of view of energetics.[1,2]

1. O. E. Garcia and N. H. Bian, Phys. Rev. E **68**, 047301 (2003).
2. O. E. Garcia, V. Naulin, A. H. Nielsen, J. Juul Rasmussen, and N. H. Bian, "Two-dimensional thermal convection in fluids and magnetized plasmas'" submitted to Physica Scripta 2005.
3. N. H. Bian and O. E. Garcia, Phys. Plasmas **12**, issue 4, to appear.

2.2.7 Shear flow generation and energetics in electromagnetic turbulence

V. Naulin, A. Kendl (Innsbruck University, Innsbruck, Austria), O.E. Garcia, A.H. Nielsen and J. Juul Rasmussen.
volker.naulin@risoe.dk

The self-consistent generation of large-scale flows by the rectification of small-scale turbulent fluctuations in magnetically confined plasmas has received strong interest during the last couple of decades. These flows may regulate the turbulence by suppressing the small-scale structures and set up transport barriers. It is generally believed that the sheared flows are instrumental in the LH transition now routinely observed in tokamaks and stellerators.

In electrostatic turbulence the Reynold stress (Re) is the source of interaction between large-scale flows and small-scale turbulence. This has been verified both in recent experiments[1] and in several numerical simulations of electrostatic turbulence. Here a strong correlation between the generations of sheared zonal flows and transport reduction is moreover clearly revealed.

In electromagnetic turbulence, which is important for finite beta plasmas as in, e.g., JET and ITER, an additional source of flow generation must be taken into account, the so-called Maxwell stress (Ma). In tokamak geometries the geodesic curvature effects, the so-called geodesic acoustic modes (GAM), will also interact with the flows in the system.

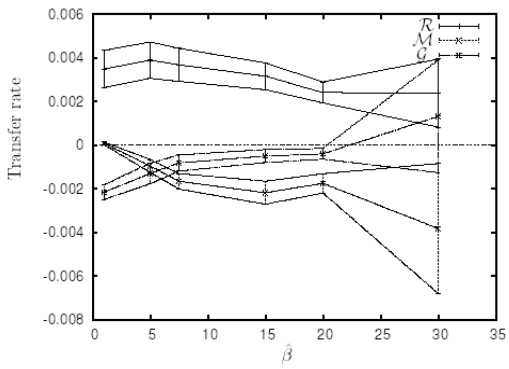

Figure 7. Dependence of the flow energy transfer rates on the scaled plasma beta.

We have examined the zonal flow generation in electromagnetic turbulence in the edge of tokamak plasmas by means of the Risø TYR code[2] governing the evolution of drift Alfvén turbulence in a 3D flux tube geometry. Covering a broad range of parameters we have revealed the relative importance of the different driving sources and sinks (Re, Ma, GAMs) for the self-consistent generation of the flows by quantifying the energy transfer into the flows due to each of these effects.

The main results have been summarised in Figure 7, where we depict the transfer rates due to three different sources/sinks. The Reynolds stress provides a drive for the flows while the electromagnetic Maxwell stress is nearly always a sink for the flow energy. In the limit high beta limit, where electromagnetic effects and Alfvén dynamics are particularly important, the Maxwell stress is found to cancel the Reynolds stress to a high degree. The GAMs, related to equilibrium pressure profile modifications due to poloidally asymmetric transport, are found to act as sinks as well as driving terms, depending on the parameter regime. For high beta cases, the GAMs are the main drive of the flow. This is also reflected in the frequency dependence of the flow, having a peak at the GAM frequency in that regime as shown in Figure 8.

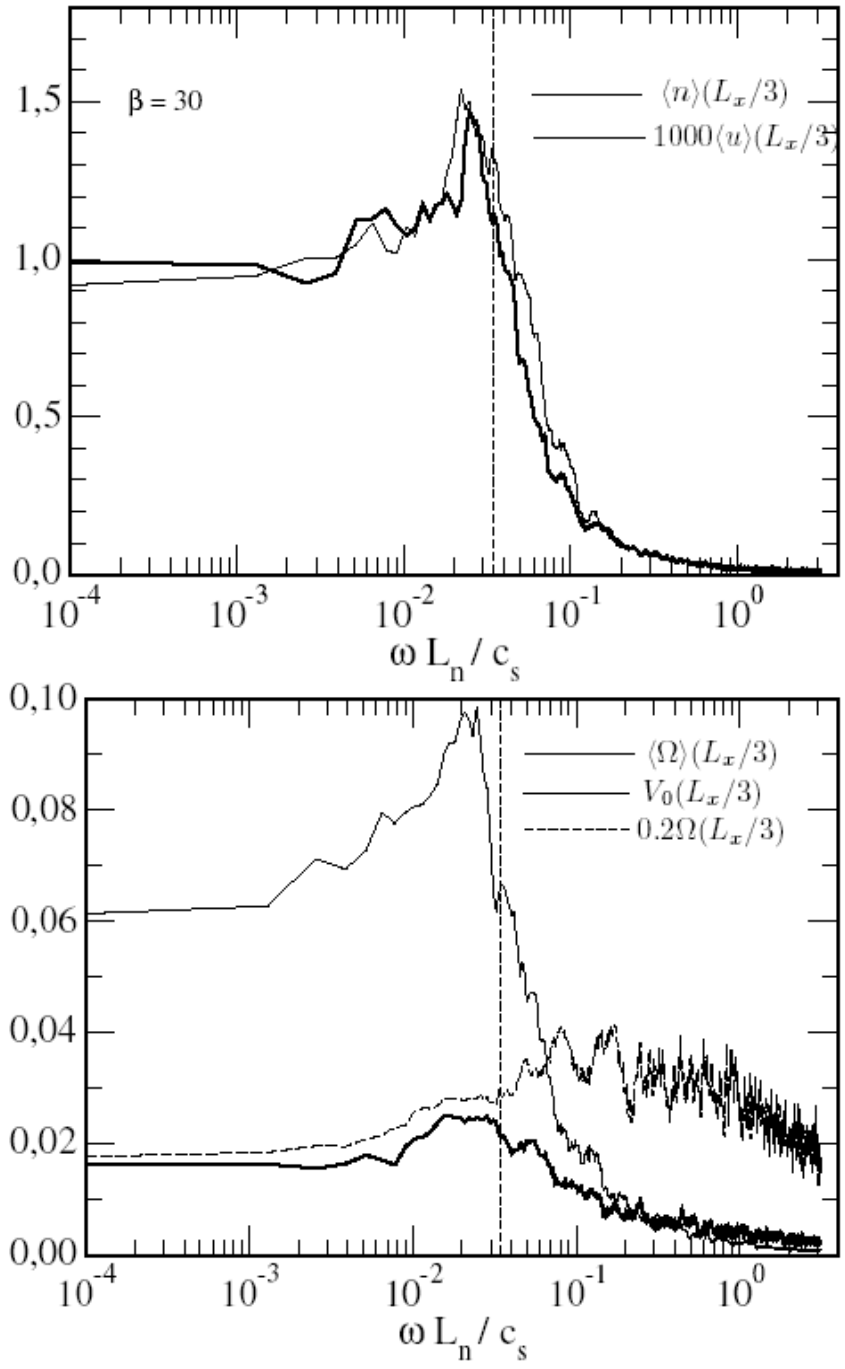

Figure 8. Frequency spectra of the quantities associated with the GAM oscillation (top) and zonal flows (bottom) for the high beta case. The vertical line shows the GAM frequency.

1. C. Hidalgo et al, Phys. Rev. Lett. **83**, 2203 (1999); Plasma Phys. Contr. Fusion **42**, Supl. 5A, A153 (2000).
2. V. Naulin, Phys. Plasmas, **10,** 4016 (2003).

2.2.8 Spatial mode structures of electrostatic drift waves in a collisional cylindrical helicon plasma

C. Schroeder, O. Grulke*, T. Klinger* (*Max-Planck-Institut für Plasmaphysik, Greifswald, Germany) and V. Naulin*
volker.naulin@risoe.dk

In a cylindrical helicon plasma, mode structures of coherent drift waves are studied in the poloidal plane, the plane perpendicular to the ambient magnetic field. The mode structures rotate at a constant angular velocity in the direction of the electron diamagnetic drift and show significant radial bending. The experimental observations, see Figure 9, have been compared with numerical solutions of a linear non-local cylindrical model for drift waves,[1] see Figure 10. In the numerical model, a transition to bended mode structures is found if the plasma collisionality is increased. This finding proves that the experimentally observed bended mode structures are the result of high electron collisionality.[2]

1. Ellis et al., Plasma Phys. **22**, 113, (1980).
2. Christiane Schröder, Olaf Grulke, Thomas Klinger and Volker Naulin, Phys. Plasmas **11**, 4249, (2004).

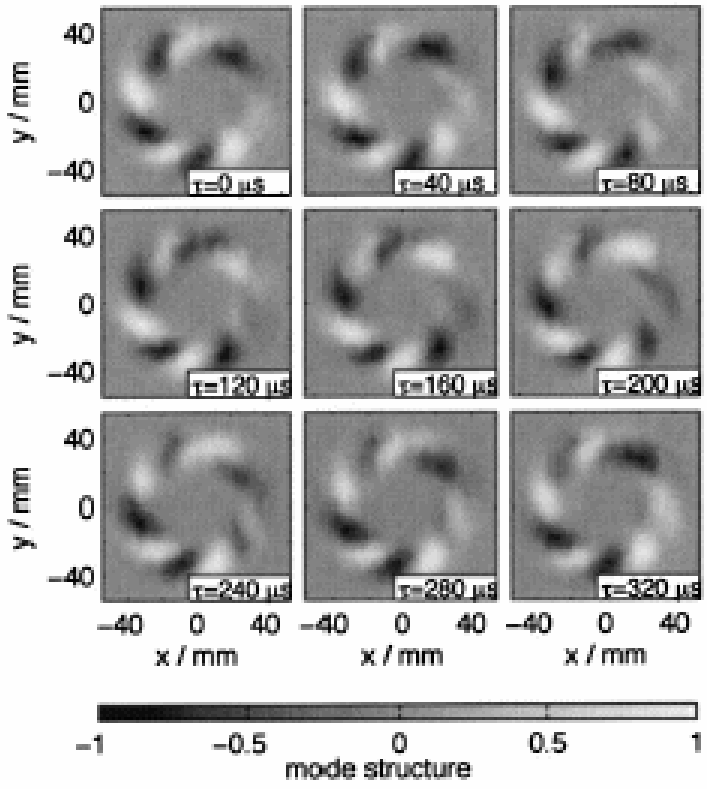

Figure 9. Poloidal mode structure obtained from the experiment.

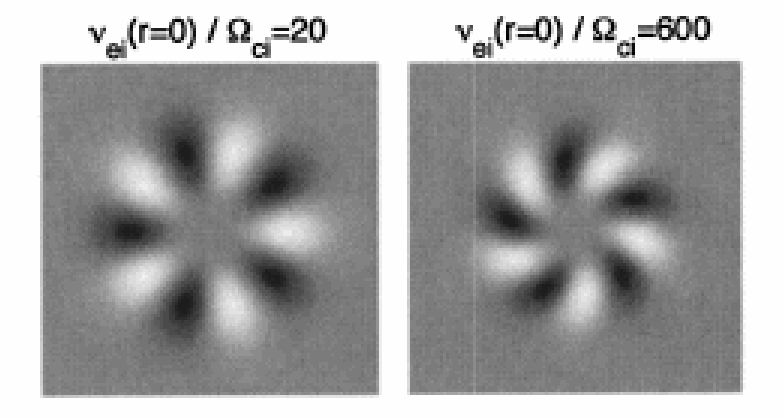

Figure 10. Poloidal mode structures obtained from the numerical model for two values of collisionality. Gaussian profiles are assumed for plasma density and Coulomb collisions, whereas the given value is the peak value.

2.3 Millimetre waves used for diagnosing fast ions in fusion plasmas

H. Bindslev, S.B. Korsholm (also at MIT Plasma Science and Fusion Center, Massachusetts, USA), F. Meo, P.K. Michelsen, S. Michelsen, S.K. Nielsen and E.L. Tsakadze
henrik.bindslev@risoe.dk
www.risoe.dk/euratom/cts

Millimetre waves, corresponding to frequencies in the 100 GHz range, permit probing and imaging on the centimetre scale and transmission of signals with bandwidths in excess of 10 GHz. Coherent sources are now available from the micro- to Megawatt range, CW. These technologies, widely used in fusion research, and in many cases specifically developed for fusion research, are now being considered for a broader range of commercial applications, including new GigaBit wireless Internet highways and wide area networks which avoid expensive trenching of optical fibres.

In the world of fusion, the millimetre waves are used extensively both as a diagnostic tool and as an actuator for manipulating the plasma locally as well as globally. Central to achieving these objectives is the fact that millimetre waves, like laser light, can be projected in narrow focused beams and, unlike laser light, the millimetre waves can interact strongly with the plasma.

At Risø we develop and exploit millimetre wave diagnostics for measuring the velocity distribution of the most energetic ions in fusion plasmas. The measurements are resolved in space on the centimetre scale and in time on the millisecond scale.

The most energetic (or fast) ions are the result of fusion reactions and auxiliary heating. Their interaction with the bulk plasma is the main mechanism by which the fusion plasmas reach and sustain the high temperatures of 100-200 million degrees Kelvin required for fusion. The considerable energy associated with the fast ions can also drive turbulence in the plasma, and degrade the confinement of the plasma and of the fast ions themselves. Understanding and controlling the dynamics of fast ions are central tasks in the development of fusion energy, and one of the main research topics for the next large fusion facility, ITER. It is a task we seek to tackle by developing and exploiting the unique diagnostic capability of millimetre wave based collective Thomson scattering (CTS).

The group has recently developed fast ion CTS diagnostics for the TEXTOR and ASDEX-Upgrade tokamaks, which are located at the Research Centre Jülich and at the Max-Planck Institute for Plasma Physics in Garching, both in Germany. Further details of this work are given in subsections 2.3.1 and 2.3.2.

Testing and commissioning of the ASDEX CTS system was completed in 2004. The first CTS measurements are awaiting installation of the new step tunable gyrotron. The CTS system for TEXTOR has been under reconstruction at Risø and was installed at TEXTOR in August. Testing, commissioning and the first ECE measurements were performed later. These projects are conducted in collaboration with MIT, the Max-Planck Institute for Plasma Physics in Garching and the TEC[1] consortium.

A feasibility study of measuring the fast ion phase space distribution in ITER by CTS and a conceptual design including a cost estimate for a measuring system was completed in 2003. The study revealed that a CTS system based on a 60 GHz probe has the highest diagnostic potential, and is the only system expected to be capable of meeting all the ITER fast ion measurement requirements with existing or near term technology. A new contract for a detailed integrated design was obtained at the end of 2004. The main purpose is to develop a design to the level allowing detailed costing and detailed design specifications of in-vessel equipment layout and subsystems for a 60 GHz CTS measuring system. Especially, the antenna system on the high field side presents problems due to limited space between and behind blanket modules. A numerical model, set up in order to study possible options, is described in subsections 2.3.7.

1. TEC: the Trilateral Euregio Cluster, comprising Association EURATOM-Forschungszentrum Jülich GmbH, Institut für Plasmaphysik, Jülich, Germany; Association EURATOM-FOM, Institute for Plasma Physics, Rijnhuizen, The Netherlands; and Association EURATOM-ERM/KMS, Belgium.

2.3.1 Collective Thomson scattering diagnostic at ASDEX Upgrade

F. Meo, H. Bindslev, S.B. Korsholm (also at MIT Plasma Science and Fusion Center, Massachusetts, USA), P.K. Michelsen, S. Michelsen, S.K. Nielsen and E.L. Tsakadze
fernando.meo@risoe.dk

The CTS diagnostic was installed at ASDEX Upgrade at the end of 2003. The system will eventually use the new ECRH system, in particular the new dual frequency gyrotron (105 GHz, 1MW, 10 sec pulse length) and the transmission lines. In 2004 the last phase of the hardware installation of the CTS system was completed. Installation of various components included new adjustable legs mounted under the receiver, the pin-switch control card that was installed and tested, and the motion of the movable mirror controller. With the help of the IPP ECRH technicians, the alignment of the quasi-optical transmission line was done using a laser. To improve the alignment in the millimetre range, a localised cold source and chopper techniques was applied whereby signals were partly measured by using one of the 1 GHz channels in the receiver and partly analysed by the LabView lock-in program. The trigger signals to the data acquisition system were incorporated with the CTS acquisition system and tested. The first ECE measurements of an ASDEX-Upgrade plasma were made. The central temperature was about 4keV. Preliminary studies comparing data from radiometry from electron cyclotron emission diagnostic have shown transmission losses larger than predicted. The most likely cause is the alignment of the CTS mirrors in the MOU box.

Figure 11. The Risø microwave receiver with the microwave horn pointing in to the hole in the MOU box.

2.3.2 Installation and commissioning of the upgraded fast ion collective Thomson scattering diagnostic at TEXTOR

S. B. Korsholm (also at MIT Plasma Science and Fusion Center, Massachusetts, USA), H. Bindslev, J. Egedal (MIT Plasma Science and Fusion Center, Massachusetts, USA), F. Meo, P. K. Michelsen, S. Michelsen, E. L. Tsakadze, E. Westerhof (FOM Institute for Plasma Physics Rijnhuizen, The Netherlands) and P. Woskov (MIT Plasma Science and Fusion Center, Massachusetts, USA)
soeren.korsholm@risoe.dk

During 2004, the major upgrade to the fast ion collective Thomson scattering (CTS) diagnostic at TEXTOR (Institut für Plasmaphysik, Jülich, Germany) became ready for installation after two years of design, construction and tests at Risø. The main constituents of the upgrade are a new quasi-optical transmission line, a new data acquisition system and an upgrade to the receiver electronics. The need for the upgrade appeared by the end of the 2000 campaign of the pilot version of the CTS system at TEXTOR. During the campaign the system was operational and obtained many useful data using a 100 kW, 0.2 s, 110 GHz gyrotron, courtesy of FOM, Holland. However, due to the location of the CTS electronics close to the tokamak and configuration changes on TEXTOR itself, noise became an increasing problem.

The details of the upgrades are the following:

(a) The receiver antenna and transmission line: a new quasi-optical transmission line has been designed and constructed. It consists of a universal polarizer and seven quasi-optical mirrors including a steerable (+/- 30° horizontal and +/- 15° vertical) plasma facing mirror.

The new transmission line allows the CTS electronics to be located on the wall of the bunker far from the tokamak (3-4 m).

(b) The electronics: The upgrade to the electronics was mainly to replace noisy components and to split the high frequency band from the centre frequency band in order to reduce the influence of possible stray light on the high frequency channels. The receiver electronics feeds 42 filters covering a frequency range that enables ion velocity distribution measurements corresponding to an ion deuterium energy range of ~ 0.5 to 200 keV. (See Section 2.2.4 *Electronics for the CTS diagnostics at ASDEX Upgrade and TEXTOR* in the annual report of 2003 for more details of the electronics in the receiver).

(c) The data acquisition system: A new National Instruments data acquisition system with 48 channels at 100 k sample/sec with 24-bit resolution has been implemented. The data acquisition system is furthermore used for controlling the polarizer and mirror motors, etc as described in subsection 2.3.4).

During one week in August 2004 the upgraded collective Thomson scattering diagnostic system was successfully installed at the TEXTOR tokamak by a team from Risø and MIT with crucial assistance from colleagues from FOM and IPP (see Figure 12, Figure 13, Figure 14 and Figure 15). This upgrade included in-vessel access for welding and mounting of three mirrors, and subsequent alignment and mapping of the orientation of the in-vessel moveable mirror. The rest of the quasi-optical transmission line was also installed as well as the receiver electronics and the data acquisition system.

During a week in November/December 2004 a team from Risø commissioned the diagnostic, debugging the system hardware and software and adapting to communicate with the IPP (timing) and FOM (gyrotron) systems. The debugging of the software was done in remote collaboration with colleagues at Risø. Following the successful systems tests, ECE measurements were performed, while also tests of the motion of the antenna were successfully performed. Preliminary analysis of the ECE data seemed to be in correspondence with IPP's ECE diagnostics.

The system is now ready for CTS operations commissioning in early 2005 using the FOM gyrotron.

Figure 12. Most of the Risø and MIT team just before the installation in August 2004.

Figure 13. The CTS antenna mounted inside the TEXTOR vessel. The antenna consists of three mirrors, of which the top left one is moveable.

Figure 14. Work on the alignment of the quasi-optical transmission line.

Figure 15. The so-called wall plate with the universal polarizer and the receiver electronics (bronze coloured box). To the left is the cabinet with further electronics and the data acquisition system.

2.3.3 Alignment and test of the quasi-optical transmission line for the TEXTOR CTS

S. Michelsen, S.B. Korsholm, E.L. Tsakadze and P. Woskov
(MIT Plasma Science and Fusion Center, Massachusetts, USA)
susanne.michelsen@risoe.dk

The quasi-optical transmission line for the CTS system at TEXTOR contains seven mirrors, one universal polariser and a circular, corrugated waveguide. During 2004 this system has been aligned with a laser system in a test bed at Risø and the transmitted mm-waves have been measured. The transmission line can be divided into three parts. The first three mirrors are mounted inside the vessel, and the waveguide couples the beam from the in-vessel mirrors to the two mirrors sitting on the outside of the vessel. The last part of the system is mounted on a 1.2 m by 1.2 m plate on the wall in the torus hall. To test the system in the laboratory at Risø, a special holder to represent the vessel was produced. Figure 16 shows this set-up with mirrors 1 to 5 together with the antenna pattern measuring system (blue area).

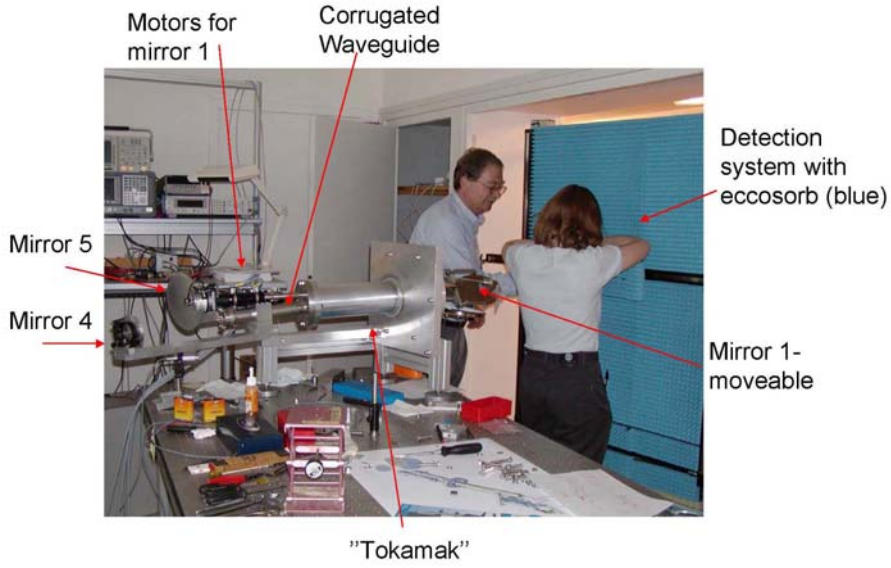

Figure 16. Alignment test.

The mm-wave beam has been successfully transmitted through the whole system from the receiver to mirror 1. Figure 17 shows the antenna pattern of the beam for one setting of mirror 1.

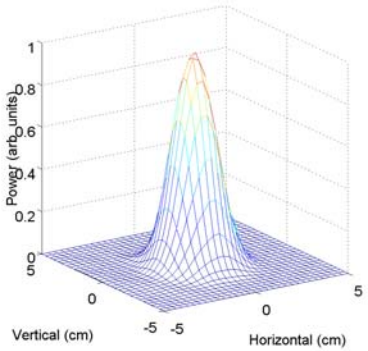

Figure 17. The antenna pattern of the beam for one setting of mirror 1.

During installation a different approach was needed since the measuring system was too large to fit into the tokamak. Instead the laser alignment was done, followed by optimisation of the mirror directions with either a cold or a hot source. This method relies on black body radiation in the mm-regime at different temperatures with respect to the radiation at room temperature. The hot source (heating element) was localised, but it had a smaller differential signal than the cold source (liquid N2). By placing the cold source in the vessel at a point localised by the laser, the mirrors were optimised so that the total loss in the transmission line was finally estimated to be approximately 2 dB. The main contribution to the loss is from the in-vessel to the out-vessel components.

We are currently building a mini-antenna pattern measuring system that can be put into the tokamak to test whether we can improve the alignment.

2.3.4 Acquisition and analysis software for collective Thomson scattering

S. K. Nielsen, F. Meo and P. K. Michelsen
stefan.kragh.nielsen@risoe.dk

The acquisition of the CTS data at the TEXTOR and ASDEX experiment (see subsections 2.3.1 and 2.3.2) requires high bit resolution and fast scan rate from a hardware point of view and a flexible user interaction. The acquisition hardware situated at ASDEX consists of 56 ADCs located on seven NI-4472 cards while the TEXTOR system consists of six cards.

Each NI-4472 contains eight 100 ksamples/sec, 24 bits resolution adc-channels.

Each system has an additional NI-6040 card with 16 channels for miscellaneous use such as VCVA switch/attenuator control and automated temperature monitoring, see Figure 18. The software, written in Labview, has been updated substantially and now includes features such as polariser and mirror control. The full acquisition system has furthermore been commissioned successfully both at ASDEX and TEXTOR.

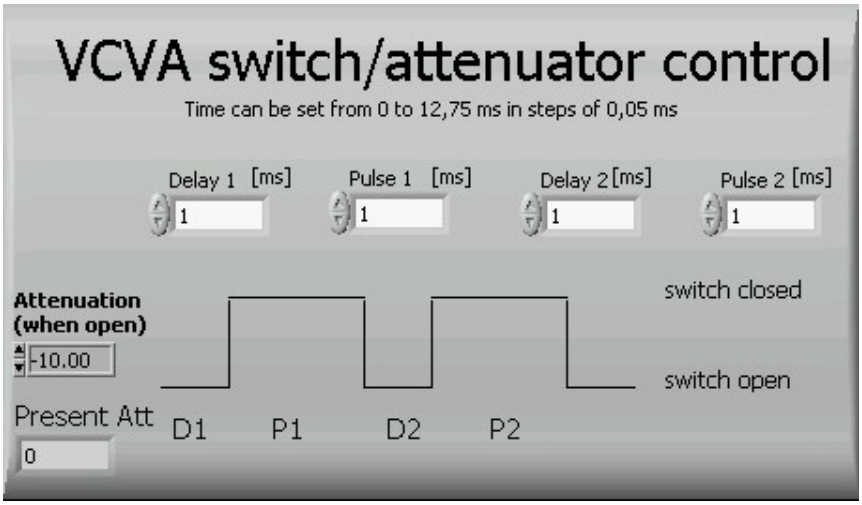

Figure 18. The VCVA switch/attenuator control in the RUDA program.

The basic function of the CTS data analysis package written for the pilot project calculates the fast ion distribution from the measured scattered radiation. It also analyses and optimises the scattering geometry to achieve optimal overlap. Keeping the core programs intact, a major upgrade to the manager routines has been made with the goal to create a generic environment to include the new data infrastructure of the pilot project as well as new CTS data, an environment that is portable to any operating systems running Matlab and FORTRAN.

2.3.5 Fast ion simulation

S. K. Nielsen and J. R. Pedersen
stefan.kragh.nielsen@risoe.dk

The understanding of fast ion dynamics is of great importance in obtaining burning, magnetically confined fusion plasmas. The confinement of the energetic alpha particles created in the fusion processes is crucial since they need to heat the bulk plasma, see Figure 19.

A numerical code for fast calculations of guiding centre orbits of energetic ions in tokamaks has been developed. The code is based on first-order orbit theory and operates in constant of motion space (energy, magnetic moment and toroidal canonical momentum). The code will be the basis of a fast ion simulation, calculating the development in time of the fast ion distribution function due to slowing down by scattering off electrons and pitch angle scattering off ions.

Figure 19. Example of fast ion orbit in a fusion device.

2.3.6 Production of high quality quasi-optical mirrors at Risø National Laboratory

E. L. Tsakadze, H. Bindslev and S. Nimb
erekle.tsakadze@risoe.dk

Among the different microwave components of the receiver antenna of the collective Thomson ccattering (CTS) diagnostic system, the quasi-optical mirrors are one of key importance. Both CTS TEXTOR and CTS ASDEX Upgrade transmission lines consist of a number of mirrors of quasi-optical quality calculated, designed and manufactured at Risø.[1,2]

The whole procedure of the mirror production starting from an idea to its actual realisation is divided into several steps (Figure 20):

(a) At the beginning the problem is formulated in MatLab, where the whole transmission line is designed and optimised to meet the set requirements. The mirror *3D* surface is calculated and can typically be ellipsoidal or hyperboloidal in shape.

(b) Obtained numerical data of the mirror surface are transferred into the graphical design tool, CATIA, in order to finalise necessary engineering details.

(c) Data from CATIA are further transferred to the PC controlling the CNC cutting tools at the Risø workshop, where the mirror is cut from the metal.

(d) The surface of the produced mirror can be carefully analysed by the surface analyser also located at the Risø workshop and obtained data are sent back to the MatLab code, where a comparison between the measured data of the mirror surface and its corresponding theoretical value is performed.

The duration of all the steps of the mirror production from MatLab to metal may be several hours depending on the mirror shape, size and sort of metal being cut. Performance of the last (d) step shows that the difference between the theoretically calculated and the experimentally measured mirror surface is typically below the 1/10 of wavelength, demonstrating high quality of the produced mirror shapes.

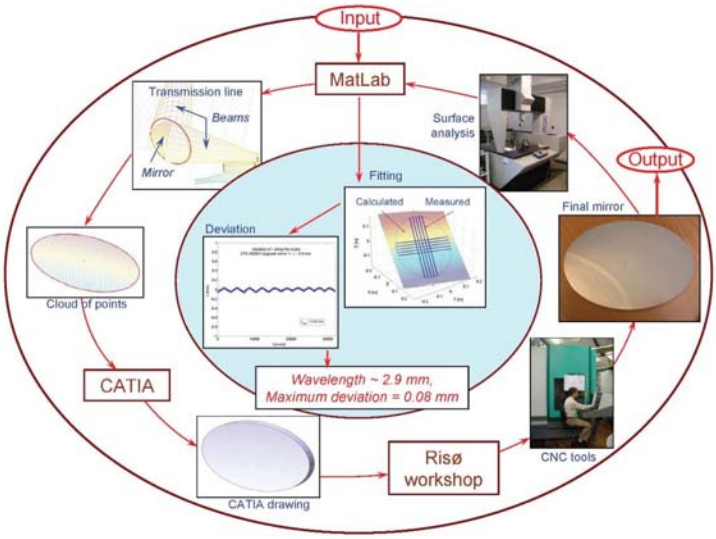

Figure 20. Production of the quasi-optical mirrors at Risø.

1. A.J.H. Donné, M.F.M. De Bock, I.G.J. Classen, M.G. Von Hellermann, K. Jakubowska, R. Jaspers, C.J. Barth, H.J. Van Der Meiden, T. Oyevaar, M.J. Van De Pol, S.K. Varshney, G. Bertschinger, W. Biel, C. Busch, K.-H. Finken, H.R. Koslowski, A. Krämer-Flecken, A. Kreter, Y. Liang, H. Oosterbeek, O. Zimmermann, G. Telesca, G. Verdoolaege, C.W. Domier, N.C. Luhmann, Jr., E. Mazzucato, T. Munsat, H. Park, M. Kantor, D. Kouprienko, A. Alexeev, S. Ohdachi, S. Korsholm, P. Woskov, H. Bindslev, F. Meo, P.K. Michelsen, S. Michelsen, S.K. Nielsen, E. Tsakadze, L. Shmaenok, "Overview of core diagnostics for TEXTOR", Fusion Science and Technology, TEXTOR special issue, **47**, n. 2, pp. 220-245, 2005.

2. S. Michelsen, S. B. Korsholm, H. Bindslev, F. Meo, P. K. Michelsen, E. L. Tsakadze, J. Egedal, P. Woskov, J. A. Hoekzema, F. Leuterer, E. Westerhof, "Fast ion millimeter wave collective Thomson scattering diagnostics on TEXTOR and ASDEX upgrades", Review of Scientific Instruments, **75**, n. 10, pp. 3634-3636, 2004.

2.3.7 Detailed integrated design of CTS for ITER

S. Michelsen, E.L. Tsakadze, H. Bindslev, A.H. Nielsen
and J. Hesthaven (Brown University, Providence, USA)
susanne.michelsen@risoe.dk

The CTS system for ITER is based on a fixed antenna system to collect scattered microwaves from different toroidal positions in the tokamak. On the high field side the slap between two blanked modules shall work as the antenna. The collected signal is reflected by two mirrors into ten horns, one for each spatial position of the scattering volume. Work has been started to optimise the mirrors, the positions of the horns and the geometry of the slap. A finite difference approach is used to model the behaviour of the slap.

The model has a maximum resolution of 20 points per wavelength and a maximal number of points of 1600x800, limited by the large amount of physical memory needed for this task. Since there is no variation in the vertical direction of the set-up the problem can be decomposed into a number of 2D finite difference problems. It is assumed that the walls of the blankets are ideal conductors and therefore the boundary conditions are $\hat{n} \times \vec{E} = 0$ and $\hat{n} \cdot \vec{H} = 0$, where n is the normal, $\vec{E}$ is the total electric field vector and $\vec{H}$ is the total magnetic field vector. Furthermore, it is necessary to use a perfect matching layer to prevent standing waves in the solution, due to reflections on the edge of the computational area.

The calculated results will be compared with experimentally obtained data using realistic geometries. Figure 21 shows an example of the total electric field calculated for a Gaussian beam that is sent through a geometry illustrated by the yellow areas. The corners of the blanket modules have been rounded to decrease the reflection from the edge.

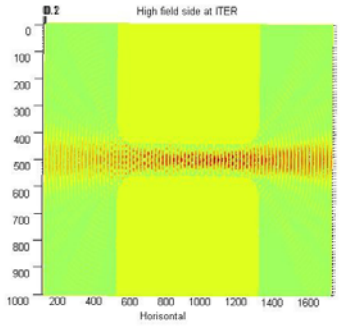

Figure 21. The total electric field is shown for the illustrated geometry (yellow areas).

2.4 Publications and conference contributions

2.4.1 International publications

Bindslev, H., Operations space diagram for ECRH and ECCD. *Nucl. Fusion* (2004) v. 44 p. 731-744

Bindslev, H.; Meo, F.; Tsakadze, E.L.; Korsholm, S.B.; Woskov, P., Feasibility study of fast ion diagnosis in ITER by collective Thomson scattering, millimeter waves to CO_2 laser. *Rev. Sci. Instrum.* (2004) v. 75 p. 3598-3600

Egedal, J.; Bindslev, H., Reconstruction of gyrotropic phase-space distributions from one-dimensional projections. *Phys. Plasmas* (2004) v. 11 p. 2191-2198

Fruh, W.G.; Nielsen, A.H., On the origin of time-dependent behaviour in a barotropically unstable shear layer. *Nonlinear Processes Geophys.* (2003) v. 10 p. 289-302

Garcia, O.E.; Naulin, V.; Nielsen, A.H.; Juul Rasmussen, J., Computations of intermittent transport in scrape-off layer plasmas. *Phys. Rev. Lett.* (2004) v. 92 p. 165003.1-165003.4

Krolikowski, W.; Bang, O.; Nikolov, N.I.; Neshev, D.; Wyller, J.; Juul Rasmussen, J.; Edmundson, D., Modulational instability, solitons and beam propagation in spatially nonlocal nonlinear media. *J. Opt. B* (2004) v. 6 p. S288-S294

LeMesurier, B.J.; Christiansen, P.L.; Gaididei, Y.B.; Juul Rasmussen, J., Beam stabilization in the two-dimensional nonlinear Schrödinger equation with an attractive potential by beam splitting and radiation. *Phys. Rev. E* (2004) v. 70 p. 046614.1-046614.7

Meo, F.; Bindslev, H.; Korsholm, S.B.; Tsakadze, E.L.; Walker, C.I.; Woskov, P.; Vayakis, G., Design of the collective Thomson scattering diagnostic for International Thermonuclear Experimental Reactor at the 60 GHz frequency range. *Rev. Sci. Instrum.* (2004) v. 75 p. 3585-3588

Michelsen, S.; Korsholm, S.B.; Bindslev, H.; Meo, F.; Michelsen, P.K.; Tsakadze, E.L.; Egedal, J.; Woskov, P.; Hoekzema, J.A.; Leuterer, F.; Westerhof, E., Fast ion millimeter wave collective Thomson scattering diagnostics on TEXTOR and ASDEX upgrades. *Rev. Sci. Instrum.* (2004) v. 75 p. 3634-3636

Naulin, V.; Juul Rasmussen, J., Aspects of turbulent transport. *Contrib. Plasma Phys.* (2004) v. 44 p. 546-551

Naulin, V.; Garcia, O.E.; Nielsen, A.H.; Juul Rasmussen, J., Statistical properties of transport in plasma turbulence. *Phys. Lett. A* (2004) v. 321 p. 355-365

Nikolov, N.I.; Neshev, D.; Krolikowski, W.; Bang, O.; Juul Rasmussen, J.; Christiansen, P.L., Attraction of nonlocal dark optical solitons. *Opt. Lett.* (2004) v. 29 p. 286-288

Ruban, V.P.; Senchenko, S.L., Local approximation for contour dynamics in effectively two-dimensional ideal electron-magnetohydrodynamic flows. *Phys. Scr.* (2004) v. 69 p. 227-233

Schröder, C.; Grulke, O.; Klinger, T.; Naulin, V., Spatial mode structures of electrostatic drift waves in a collisional cylindrical helicon plasma. *Phys. Plasmas* (2004) v. 11 p. 4249-4253

Tsakadze, E.L.; Ostrikov, K.N.; Tsakadze, Z.L.; Vladimirov, S.V.; Xu, S., Magnetic fields and uniformity of radio frequency power deposition in low-frequency inductively coupled plasmas with crossed internal oscillating currents. *Phys. Plasmas* (2004) v. 11 p. 3915-3924

Tsakadze, E.L.; Ostrikov, K.N.; Tsakadze, Z.L.; Xu, S., Generation of uniform plasmas by crossed internal oscillating current sheets: Key concepts and experimental verification. *J. Appl. Phys.* (2005) v. 97 p. 013301.1-013301.10

2.4.2 Danish publications

Bindslev, H.; Singh, B.N (eds.), Association Euratom - Risø National Laboratory annual progress report 2003. Risø-R-1468(EN) (2004) 60 p. www.risoe.dk/rispubl/ofd/ris-r-1468.htm

Senchenko, S.L., Stationary viscous flows with free surface and vortex structures in plasmas flows. (Technical University of Denmark, Lyngby, 2004) 119 p. (ph.d. thesis)

2.4.3 Conference lectures

Balan, P.; Figueiredo, H.F.C.; Galvao, R.M.O.; Ionita, C.; Naulin, V.; Juul Rasmussen, J.; Schrittwieser, R.; Silva, C.G.; Varandas, C., Measurements of the fluctuation-induced flux and the Reynolds stress in the edge region of ISTTOK. In: Contributed papers. 31. European Physical Society conference on plasma physics, London (GB), 28 Jun - 2 Jul 2004. (European Physical Society, Paris, 2004) (Europhysics Conference Abstracts, vol. 28G) P-5.119 (4 p.)

Bindslev, H.; Garcia, O.E.; Naulin, V.; Nielsen, A.H.; Juul Rasmussen, J., Transport and zonal flow energetics in plasma edge turbulence (poster). In: Contributed papers. 31. European Physical Society conference on plasma physics, London (GB), 28 Jun - 2 Jul 2004. (European Physical Society, Paris, 2004) (Europhysics Conference Abstracts, vol. 28B) P-5.143 (4 p.)

Bindslev, H.; Meo, F.; Korsholm, S.B.; Egedal, J.; Michelsen, S.; Nielsen, S.K.; Woskov, P., Diagnosing fast ions in ITER by collective Thomson scattering (poster). In: Contributed papers. 31. European Physical Society conference on plasma physics, London (GB), 28 Jun - 2 Jul 2004. (European Physical Society, Paris, 2004) (Europhysics Conference Abstracts, vol. 28B) P-5.144 (4 p.)

Fateev, A.; Leipold, F.; Kusano, Y.; Stenum, B.; Tsakadze, E.L.; Bindslev, H., Plasma chemistry in an atmospheric ressure Ar/NH_3 dielectric barrier discharge (oral presentation). In: HAKONE IX (CD-ROM). 9. International symposium on high pressure low temperature plasma chemistry, Padova (IT), 23-27 Aug 2004. (University of Padua, Padua, 2004) 8 p.

Garcia, O.E.; Naulin, V.; Nielsen, A.H.; Juul Rasmussen, J., Intermittent transport in edge plasmas. In: Contributed papers [on the internet]. 12. International congress on plasma physics, Nice (FR), 25-29 Oct 2004. (CEA, 2004) 6 p. hal.ccsd.cnrs.fr/ccsd-00001828

Leipold, F.; Fateev, A.; Kusano, Y.; Stenum, B.; Tsakadze, E.; Bindslev, H., Detection of NH_2 and NH in atmospheric pressure Ar/NH_3 dielectric barrier discharge. In: Proceedings. 4. International symposium on non-thermal plasma technology for pollution control and sustainable energy development (ISNTPT-4), Panama City Beach, FL (US), 10-14 May 2004. Locke, B.R. (ed.), (Florida State University and Florida Agricultural and Mechanical University, Tallahassee, 2004) p. 69-72

Michelsen, S.; Bindslev, H.; Egedal, J.; Hoekzema, J.A.; Korsholm, S.B.; Leuterer, F.; Meo, F.; Michelsen, P.K.; Nielsen, S.K.; Tsakadze, E.L.; Westerhof, E.; Woskov, P., Fast ion millimeter wave CTS diagnostics on TEXTOR and ASDEX upgrade (poster). In: Contributed papers. 31. European Physical Society conference on plasma physics, London (GB), 28 Jun - 2 Jul 2004. (European Physical Society, Paris, 2004) (Europhysics Conference Abstracts, vol. 28B) P-1.131 (4 p.)

Naulin, V.; Garcia, O.E.; Nielsen, A.H.; Juul Rasmussen, J.; Bindslev, H., Impurity transport in 3D plasma edge turbulence (poster). In: Contributed papers. 31. European Physical Society conference on plasma physics, London (GB), 28 Jun - 2 Jul 2004. (European Physical Society, Paris, 2004) (Europhysics Conference Abstracts, vol. 28B) P-4.141 (4 p.)

Naulin, V.; Wood, M.P.; Juul Rasmussen, J., Impurity transport in plasma edge turbulence. In: Contributed papers [on the internet]. 12. International congress on plasma physics, Nice (FR), 25-29 Oct 2004. (CEA, 2004) 6 p. hal.ccsd.cnrs.fr/ccsd-00001826

2.4.4 Publications for a broader readership

Andersen, A.; Bohr, T.; Stenum, B.; Juul Rasmussen, J.; Lautrup, B.; Ernebjerg, M., Badekarshvirvlens anatomi. Nat. Verden (2004) v. 87 (no.7/8) p. 28-33

Jensen, V.O., Solens energikilde ned på Jorden. Jyllands-Posten Søndag (2004) (no.28 Mar 2004)

2.4.5 Unpublished Danish lectures incl. published abstracts

Bindslev, H., Modificering af materialer ved hjælp af plasma. Konference: Materialer og innovation i oplevelsessamfundet, Risø (DK), 22 Nov 2004. Unpublished.

Jensen, V.O., Hvordan kan menneskeheden få sit energibehov dækket i fremtiden?. Inspirationsmøde i Akademiet for den Tredje Alder (A-3-A), København (DK), 20 Oct 2004. Unpublished.

Jensen, V.O., ITER's rolle i fusionsforskningen. Videnberedskabsseminar, Risø (DK), 15 Apr 2004. Unpublished.

2.4.6 Unpublished international lectures incl. published abstracts

Bindslev, H.; Meo, F.; Korsholm, S.B.; Tsakadze, E.; Woskov, P., Feasibility study of fast ion diagnosis in ITER by collective Thomson scattering, mm-waves to CO_2 laser. 15. Topical conference on high-temperature plasma diagnostics, San Dieto, CA (US), 19-22 Apr 2004. Unpublished. Abstract available

Bindslev, H.; Meo, F.; Korsholm, S.B.; Woskov, P.; Egedal, J., Fast ion CTS for ITER. 15. Topical conference on high-temperature plasma diagnostics, San Dieto, CA (US), 19-22 Apr 2004. Unpublished. Abstract available

Egedal, J.; Bindslev, H.; Woskov, P., Calculation of beam ion distributions in ITER and their impact on alpha-particle measurements by collective Thomson scattering (poster). 45. Annual meeting of the Division of Plasma Physics, American Physical Society, Albuquerque, NM (US), 27-31 Oct 2003. Unpublished. Abstract available

Egedal, J.; Woskov, P.; Bindslev, H., Calculation of beam ion distributions in ITER and their impact on alpha-particle measurements by collective Thomson scattering. 15. Topical conference on high-temperature plasma diagnostics, San Dieto, CA (US), 19-22 Apr 2004. Unpublished. Abstract available

Garcia, O.E., Intermittent transport in magnetized plasmas with differential rotation. In: Program and abstracts. 3. Nordic symposium on plasma physics, Oslo (NO), 4-7 Oct 2004. (Norwegian Centre for Advanced Study, Oslo, 2004) p. 12

Juul Rasmussen, J., Turbulent equipartition and anomalous transport in electrostatic plasma turbulence. Seminar series on transport of matter and radiation, Space Research Institute, Moscow (RU), 9 Jun 2004. Unpublished.

Juul Rasmussen, J., Particle diffusion and density flux in low-frequency, electrostatic plasma turbulence. Seminar series on transport of matter and radiation, Space Research Institute, Moscow (RU), 11 Jun 2004. Unpublished.

Juul Rasmussen, J.; Bang, O.; Krolikowski, W.Z.; Wyller, J., Nonlinear wave propagation in nonlocal media (invited talk). In: Abstracts. 2. International conference on frontiers of nonlinear physics, Nizhny Novgorod - St. Petersburg (RU), 5-12 Jul 2004. (Russian Academy of Sciences, Nizhny Novgorod (RU), 2004) p. 40

Juul Rasmussen, J.; Garcia, O.E.; Naulin, V.; Nielsen, A.H.; Stenum, B.; Bokhoven, L.J.A. van; Konijnenberg, J. van de; Delaux, S., Zonal flow generation in rotating fluids and magnetized plasmas. In: Program and abstracts. 3. Nordic symposium on plasma physics, Oslo (NO), 4-7 Oct 2004. (Norwegian Centre for Advanced Study, Oslo, 2004) p. 9-10

Korsholm, S.B.; Bindslev, H.; Meo, F.; Michelsen, S.; Michelsen, P.K.; Nielsen, S.K.; Tsakadze, E.L.; Egedal, J.; Woskov, P.; Hoekzema, J.; Leuterer, F.; Westerhof, E., Fast ion millimeter wave CTS diagnostic installation activities on TEXTOR and ASDEX upgrade (poster). In: Book of abstracts. 46. Annual meeting of the Division of Plasma Physics, American Physical Society, Savannah, GA (US), 15-19 Nov 2004. (American Physical Society, Division of Plasma Plysics, 2004) BP1.096

Krolikowski, W.; Nikolov, N.I.; Bang, O.; Neshev, D.; Wyller, J.; Juul Rasmussen, J.; Edmondson, D., Optical beams and spatial solitons in nonlocal nonlinear media (oral presentation). CLEO/IQEC conference on lasers and electro optics / International quantum electronics conference, San Francisco, CA (US), 16-21 May 2004. Unpublished.

Kusano, Y.; Leipold, F.; Fateev, A.; Stenum, B.; Tsakadze, E.L.; Egsgaard, H.; Bindslev, H., Production of ammonia radicals in a dielectric barrier discharge and their injection for denitrification. In: Book of abstracts. 9. International conference on plasma surface engineering, Garmisch-Partenkirchen (DE), 13-17 Sep 2004. (VDI-Technology Center, Düsseldorf, 2004) 1 p.

Meo, F.; Bindslev, H.; Korsholm, S.B.; Tsakadze, E.; Walker, C.; Woskov, P., Design of the collective Thomson scattering diagnostic for ITER at the 60 GHz frequency range. 15. Topical conference on high-temperature plasma diagnostics, San Dieto, CA (US), 19-22 Apr 2004. Unpublished. Abstract available

Michelsen, S.; Bindslev, H.; Egedal, J.; Hoekzema, J.A.; Korsholm, S.B.; Leuterer, F.; Meo, F.; Michelsen, P.K.; Tsakadze, E.L.; Westerhof, E.; Woskov, P., Fast ion millimeter wave CTS diagnostics on TEXTOR and ASDEX upgrade. 15. Topical conference on high-temperature plasma diagnostics, San Dieto, CA (US), 19-22 Apr 2004. Unpublished. Paper available

Naulin, V., Anomalous impurity pinch in edge turbulence. Max Planck Institute for Plasma Physics Theory seminar, Ringberg (DE), 4-12 Nov 2004. Unpublished.

Naulin, V., Modeling control of low frequency plasma turbulence (invited talk). Hamiltonian systems, control and plasma physics (HSCoPP 04), Frejus (FR), 21-23 Oct 2004. Unpublished.

Naulin, V., Transport and mixing of passive fields in compressible plasma turbulence. In: Abstracts. 2. International conference on frontiers of nonlinear physics, Nizhny Novgorod - St. Petersburg (RU), 5-12 Jul 2004. (Russian Academy of Sciences, Nizhny Novgorod (RU), 2004) p. 38

Naulin, V.; Garcia, O.E.; Kendl, A.; Nielsen, A.H.; Juul Rasmussen, J., Zonal flow generation mechanisms in drift-Alfvén turbulence. 9. EU-US transport task force workshop, Varenna (IT), 6-9 Sep 2004. Unpublished.

Naulin, V.; Juul Rasmussen, J.; Wood, M.P., Trace tritium transport in Tokamak edge turbulence (invited talk). 4. Symposium des SFB 591, Bad Honnef (DE), 1-3 Dec 2004. Unpublished.

Naulin, V.; Juul Rasmussen, J.; Wood, M.P., Trace tritium transport in Tokamak edge turbulence. Kolloquium, LPMI, University Henri Poincare, Nany (FR), 9 Jun 2004. Unpublished.

Naulin, V.; Juul Rasmussen, J.; Wood, M.P., Anomalous impurity pinch in edge turbulence. In: Program and abstracts. 3. Nordic symposium on plasma physics, Oslo (NO), 4-7 Oct 2004. (Norwegian Centre for Advanced Study, Oslo, 2004) p. 13-14

Naulin, V.; Juul Rasmussen, J.; Wood, M.P., Pinch effects in turbulent impurity transport. Joint Lausanne Varenna workshop on plasma theory, Varenna (IT), 30 Aug - 4 Sep 2004. Unpublished.

Naulin, V.; Juul Rasmussen, J., Impurity transport in the edge. TF-T workshop at JET, Abingdon (GB), 27-30 Jan 2004. Unpublished.

Nielsen, A.H.; Garcia, O.E.; Naulin, V.; Grulke, O.; Juul Rasmussen, J., 2D simulation of blob propagation in edge and SOL. In: Program and abstracts. 3. Nordic symposium on plasma physics, Oslo (NO), 4-7 Oct 2004. (Norwegian Centre for Advanced Study, Oslo, 2004) p. 14

Nielsen, S.K., Fast ion measured by collective Thomson scattering (poster). 41. Culham Plasma Physics Summer School, Oxfordshire (GB), 19-30 Jul 2004. Unpublished.

Nikolov, N.I.; Neshev, D.; Bang, O.; Krolikowski, W.; Wyller, J., A nonlocal description of two-color parametric solitons (poster and oral presentation). Nonlinear guided waves and their applications topical meeting, Toronto (CA), 28-31 Mar 2004. Unpublished.

Sørensen, T.; Nikolov, N.I.; Bang, O.; Bjarklev, A.; Hougaard, K.G.; Hansen, K.P., Dispersion engineered cob-web photonic crystal fibers for efficient supercontinuum genertion. 2004 optical fiber communication conference, Los Angeles, CA (US), 22-27 Feb 2004. Unpublished.

Sørensen, T.; Nikolov, N.I.; Bang, O.; Bjarklev, A.; Hougaard, K.G.; Hansen, K.P.; Juul Rasmussen, J., Cob-web microstructured fibers optimized for supercontinuum generation with picosecond pulses (oral presentation). Nonlinear guided wves and their applications, topical meeting, Toronto (CA), 28-31 Mar 2004. Unpublished.

Tsakadze, E.L.; Ostrikov, K.; Tsakadze, K.; Xu, S., Internal oscillating current-sustrained of plasmas: Parameters, stability, and potential for surface engineering (oral presentation). In: Book of abstracts. 9. International conference on plasma surface engineering, Garmisch-Partenkirchen (DE), 13-17 Sep 2004. (VDI-Technology Center, Düsseldorf, 2004) 1 p.

Tsakadze, Z.; Ostrikov, K.; Xu, S.; Tsakadze, E., Generation of high-density, uniform plasmas by internal RF current sheets: Key concepts and experimental verification. 56. Gaseous Electronics Conference, San Francisco, CA (US), 21-24 Oct 2003. Unpublished. Abstract available

Wyller, J.; Krolikowski, W.; Petersen, D.E.; Bang, O.; Juul Rasmussen, J., Modulational instability in a nonlocal χ^{2} - model (poster). SIAM conference on nonlinear waves and coherent structures, Orlando, FL (US), 2-5 Oct 2004. Unpublished.

2.4.7 Internal reports

Bindslev, H.; Meo, F.; Korsholm, S., ITER fast ion collective Thomson scattering. Feasibility study and conceptual design. (2003) 196 p.

3. Fusion technology

3.1 Introduction

The work reported in this section has been carried out in the Materials Research Department. The overall objective of the research activities in this area is to determine the impact of neutron irradiation on physical and mechanical properties of metals and alloys, so that appropriate materials can be chosen for their application in irradiation environment (e.g. in fusion reactor). Various experimental techniques are employed to study different aspects of the microstructural evolution during irradiation and the resulting consequences of the post-irradiation physical and mechanical properties of metals and alloys. Calculations and computer simulations are performed to understand the evolution of surviving defects and their clusters in collision cascades. The kinetics of defect accumulation during irradiation and the influence of irradiation-induced defects and their clusters on the deformation behaviour of irradiated metals and alloys are studies theoretically. In the following, the main results of these activities are highlighted.

3.2 Next step technology

3.2.1 In-reactor creep-fatigue cyclic testing of CuCrZr alloy[1]

B.N. Singh, S. Tähtinem, P. Moilanen* (VTT Industrial Systems (Association EURATOM-TEKES), Espoo, Finland)), P. Jacquet** and J. Dekeyser** (Reactor Experiment Department, SCK.CEN, Mol, Belgium)*

At present it seems almost certain that the precipitation hardened CuCrZr alloy will be used both in the first wall and divertor components of ITER. In the reactor vessel, this alloy will be exposed to a relatively high flux of 14 MeV neutrons and will experience thermo-mechanical cyclic loading as a result of the cyclic nature of the plasma burn operations of the system. Because of the "plasma-on" and "plasma-off" mode of operation, the deformation behaviour of the alloy is likely to be modified. This kind of cyclic loading would induce not only fatigue damage but also make the material creep during the operation. Not much is known at present about the impact of this complicated mode of deformation on the mechanical performance of metals and alloys particularly in the environment of intense neutron irradiation. The limited amount of experimental results on creep-fatigue experiments carried out on the unirradiated CuCrZr alloy (and in the absence of neutron irradiation) have shown, on the other hand, that hold-times are damaging and shorten the number of cycles to failure.

The materials employed in the first wall and the divertor components of ITER will experience thermo-mechanical stresses and displacement damage concurrently. This may modify the creep-fatigue deformation response of the material significantly. In order to make a realistic evaluation of the response of materials under these conditions, an experimental programme was initiated with the objective of carrying out creep-fatigue experiments directly in the environment of neutrons in the BR-2 reactor at Mol (Belgium). In order to carry out

[1] TW3 – TVM - COFAT

such tests it was necessary to design a new test facility in which it was possible to reverse the loading mode from tension to compression in a cyclic fashion and with the possibility of implementing a certain hold-time both on the tension and compression sides of the loading cycle. This required a very robust and mechanically stable test module where specimen alignment could be maintained within a very narrow margin over a period of 20 days covering several thousands of loading cycles. This also meant that the design of the specimen had to be changed so that the specimen could be firmly gripped in the test module and should not bend during the test. The size and the geometry of the specimen are shown in Figure 22.

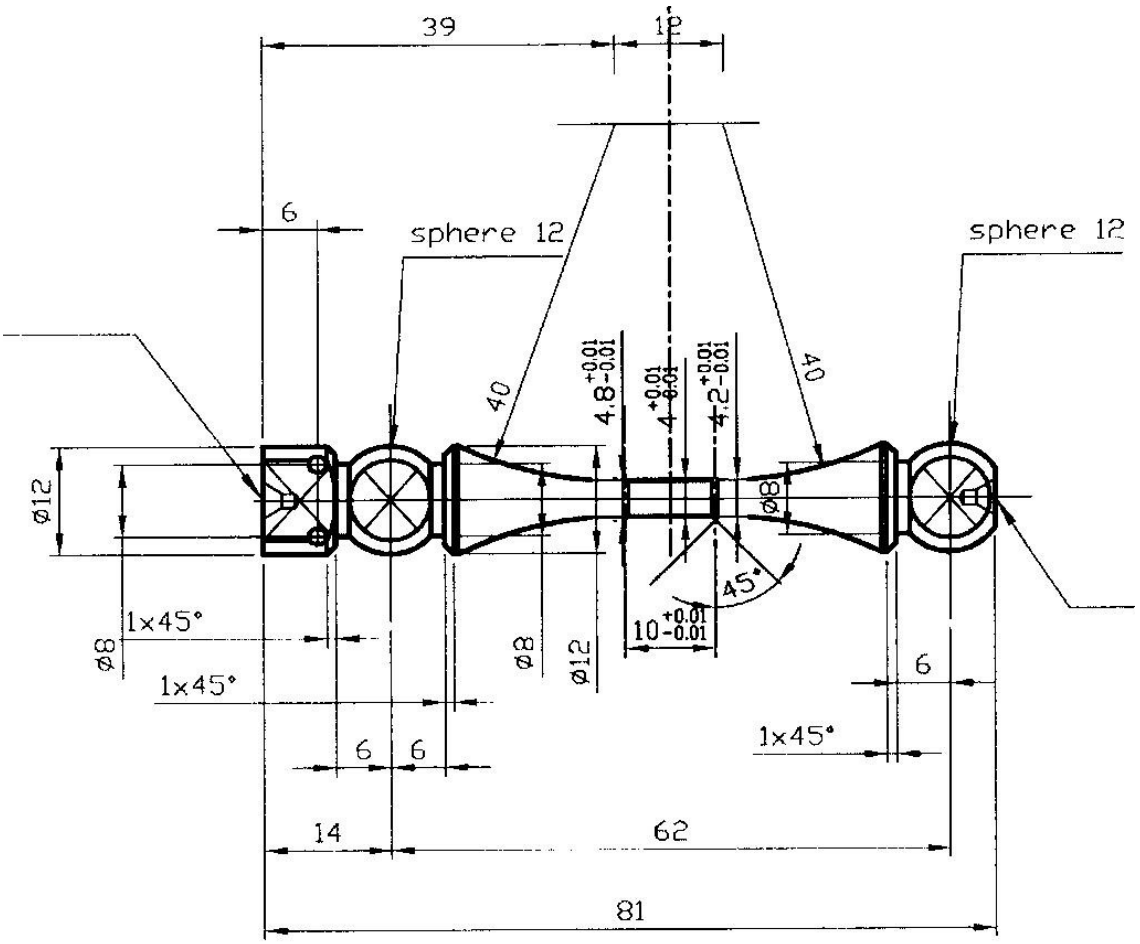

Figure 22. Size and geometry of specially designed specimen for in-reactor creep-fatigue tests.

The test facility consists of a pneumatic fatigue test module and a servo-controlled pressure-adjusting loop. The pressure-adjusting loop operates on a continuous flow of helium gas. The basic principle of the creep-fatigue test module is based on the use of two pneumatic bellows to introduce stress/strain and a linear variable differential transformer (LVDT) sensor to measure the resulting extension of the grange length of the creep-fatigue specimen between the two connecting rings (see Figure 23). The strain measured by the LVDT has been calibrated against the strain measured by strain gauges. The strain measured between the two connection rings is used to control the pre-determined constant strain amplitude throughout the whole test. It should be pointed out that one bellows is used to induce tension whereas the other bellows induces compression (see Figure 24a). Figure 24b illustrates that the present design of the test module can be used to perform a reliable creep-fatigue test with a certain hold-time.

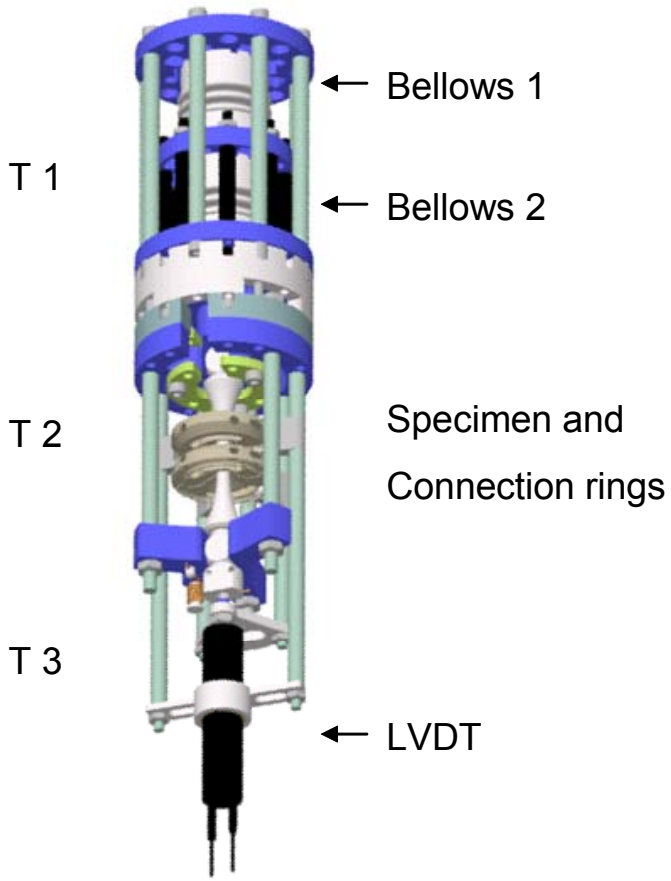

Figure 23. Assembly of a part of the test module showing bellows, specimen and connection rings. Positions of the three thermocouples to be used during the tests are also marked.

Two such test modules have been fabricated and loaded into an instrumented rig for carrying out reference tests in air and in water. These calibrated test modules will be used for the in-reactor creep-fatigue tests.

3.2.2 Creep-fatigue cyclic deformation behaviour of unirradiated and irradiated CuCrZr alloy[2]

B.N. Singh and B.S. Johansen

Since one of the precipitation hardened CuCrZr alloys is most likely to be used in the first wall and diverter components of ITER, various aspects of the effects of precipitate microstructure and neutron irradiation on its mechanical properties are being investigated. Because of the cyclic nature of the plasma burn operations expected in ITER, the CuCrZr alloy employed in the first wall as well as diverter components will experience thermomechanical cyclic loading. This kind of cyclic loading would induce not only fatigue damage but would also make the material creep during the operation. Preliminary creep-fatigue experiments on the unirradiated CuCrZr alloy at room temperature have indicated that

[2] TW2 – TVM – CUCFA and TW3 – TVM – CUCFAZ

the application of a certain hold-time between the fatigue ccles lowers the number of cycles to failure. The work was extended to include investigations of the effect of heat treatment and irradiation and test temperatures on the creep-fatigue behaviour of CuCrZr alloy.

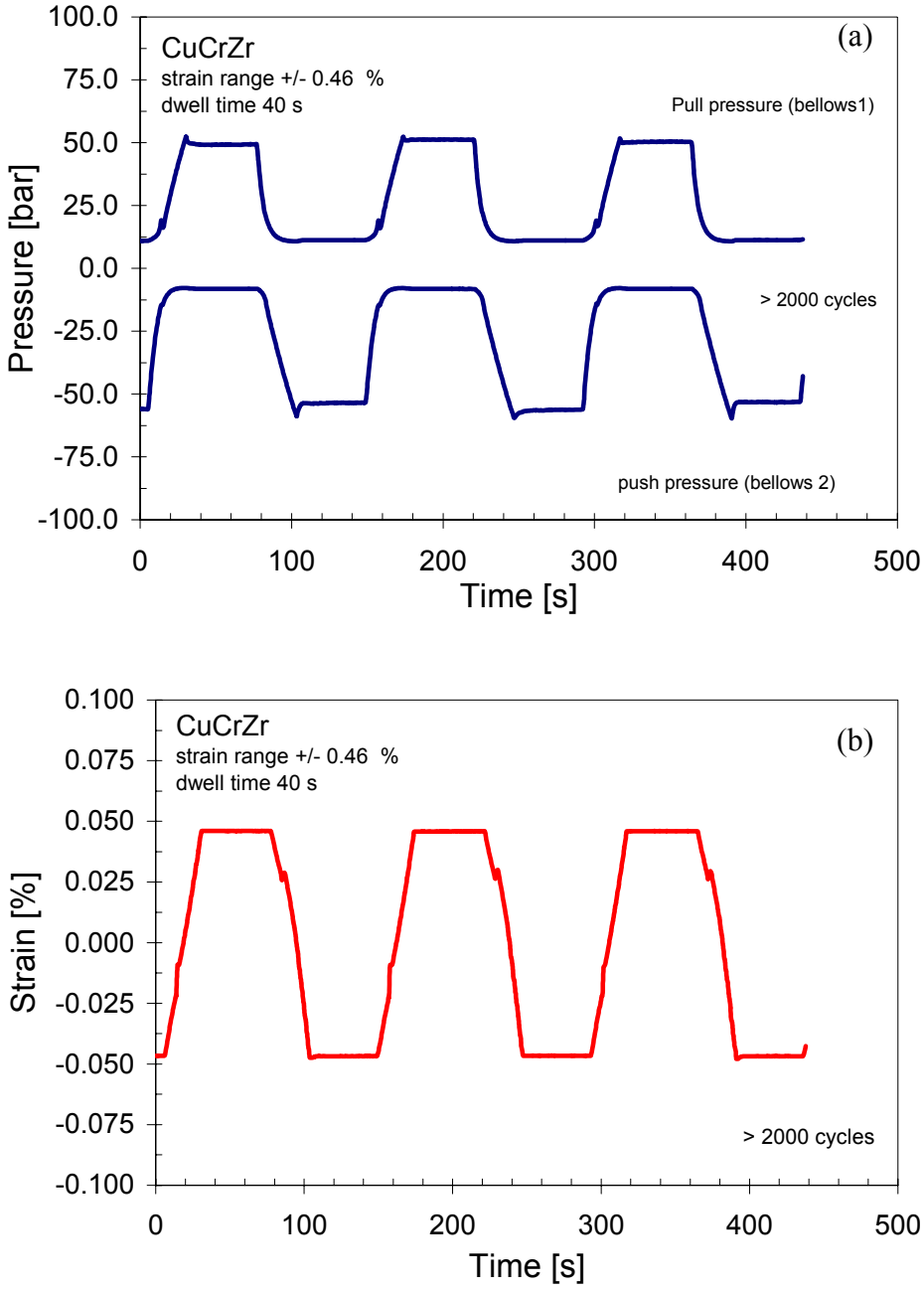

Figure 24. An example of the pressure and strain response af a specimen as a function of time during a creep-fatigue test performed using the test module shown in Figure 23. The test was carried out at room temperature on a specimen (Figure 22) of CuCrZr alloy.

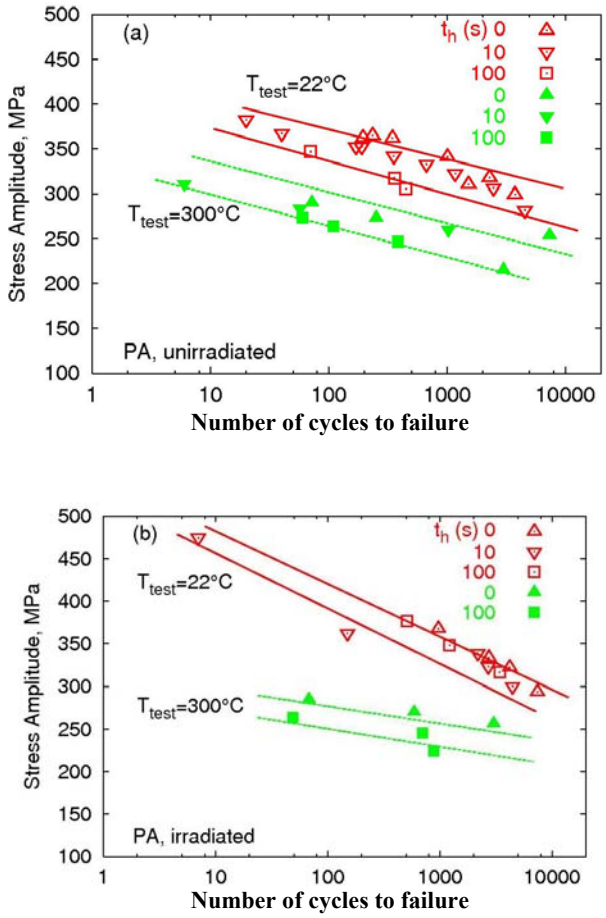

Figure 25. Number of cycles for failure (N_f) as a function of stress amplitude in creep-fatigue tests carried out on the prime aged (PA) CuCrZr alloy at 22 and 300°C in the (a) unirradiated and (b) irradiated (at 60 and 300°C to 0.2-0.3 dpa) conditions. Results are shown for 0, 10 and 100s holdtimes (t_h).

A number of fatigue specimens were fabricated. Subsequently, some of these specimens were prime aged (PA) and some others were over-aged at 600°C for 1 h. Both types of specimens were neutron irradiated in the BR-2 reactor at Mol (Belgium) to a displacement dose level of 0.2 - 0.3 dpa at 60 and 300°C. The damage rate during irradiation was about 5 x 10^{-8} dpa/s. Both the prime aged and the over-aged specimens were creep-fatigue tested at 60 and 300°C (in vacuum) in the unirradiated as well as irradiated conditions. The loading cycles were always fully reversed (i.e. R = -1) and had a frequency of 0.25 Hz. Tests were conducted with tension and compression holdtime (t_h) of 0, 10 and 100 s. The specimens were cycled to failure. The variations of the number of cycles to failure, N_f, with the stress amplitude for the prime aged (PA) CuCrZr alloy tested at 22 and 300°C is shown in Figure 25a for the unirradiated and Figure 25b for the irradiated specimens. Similar variations for the overaged CuCrZr alloy tested at 22 and 300°C are shown in Figure 26(a) and Figure 26(b) for the unirradiated an irradiated specimens. The results presented in Figure 25 and Figure 26 clearly demonstrate that the lifetime of the CuCrZr alloy both in the prime aged and overaged conditions is strongly dependent on the test temperature. The effect is even stronger in the case of irradiated conditions.

The comparison of results shown in Figure 25 and Figure 26 for the prime aged and the over-aged CuCrZr alloy demonstrates that the overaging of CuCrZr alloy at 600 °C for 1 h reduces the lifetime (i.e. N_f at a given stress amplitude) signigficantly. This tendency persists even in the materials that are tested after irradiation.

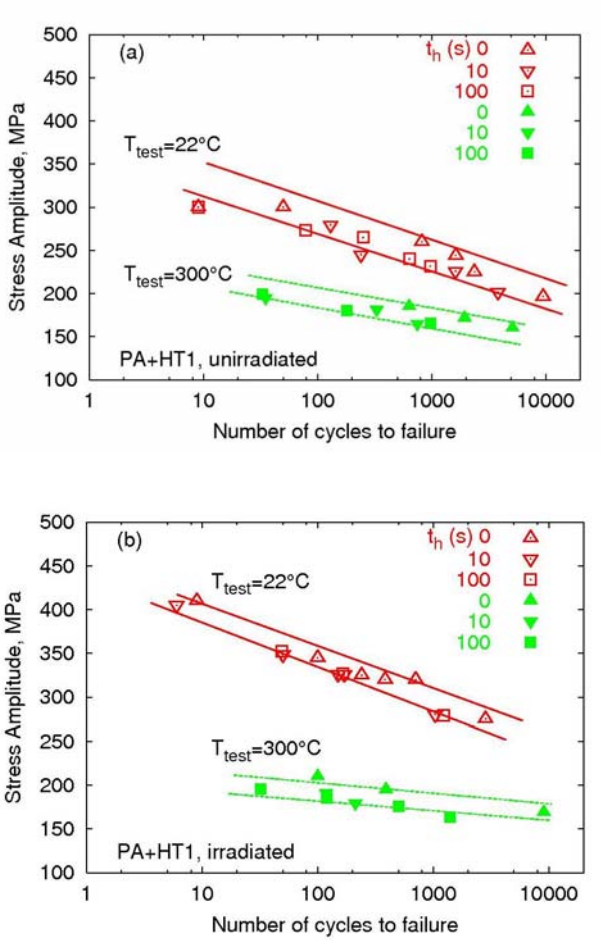

Figure 26. Same as in Figure 25 but for the overaged (600°C/1h) CuCrZr alloy specimens tested at 22 and 300 °C in the (a) unirradiated and (b) irradiated (60 and 300°C, 0.2-0.3 dpa) conditions. Results are shown for 0, 10 and 100s holdtimes (t_h).

The irradiation at 60°C increases the number of cycles to failure (at a given stress amplitude) considerably in the case of the prime aged as well as over-aged conditions. This increase appears to be larger in the case of the over-aged specimens than that in the prime aged specimens. Irradiations at 300°C, on the other hand, do not appear to have any noticeable effects on the lifetime.

As regards the effect of hols time, all the results presented here illustrate a general trend that the application of a hold-time always reduces the lifetime. The hold-time does not appear to have any significant reduction in the lifetime of specimens irradiated at 60 °C and tested at 22°C. However, in the unirradiated condition, the lifetime of both prime-aged and over-aged specimens is noticeably reduced due to hold-time. Both the prime-aged and over-aged specimens irradiated and tested at 300°C exhibit a significant reduction in the lifetime due to the application of a hold-time.

3.2.3 Effect of Irradiation on mechanical properties of Titanium alloys[3]

B.N. Singh and B.S. Johansen

The (α + β) Ti-alloy (Ti 6Al 4V) is still being considered as a candidate material for the flexible connectors between the blanket modules and the back plate of ITER. Since not much is known about the effect of neutron irradiation on the phase stability and mechanical properties of this alloy, screening investigations were carried out to determine the response of this alloy to neutron irradiation at 50 and 350°C to a dose level of 0.3 dpa. The results of these investigations have been reported earlier[4]. Recently, it was decided to carry out some additional irradiations and testing at intermediate temperatures and to different dose levels.

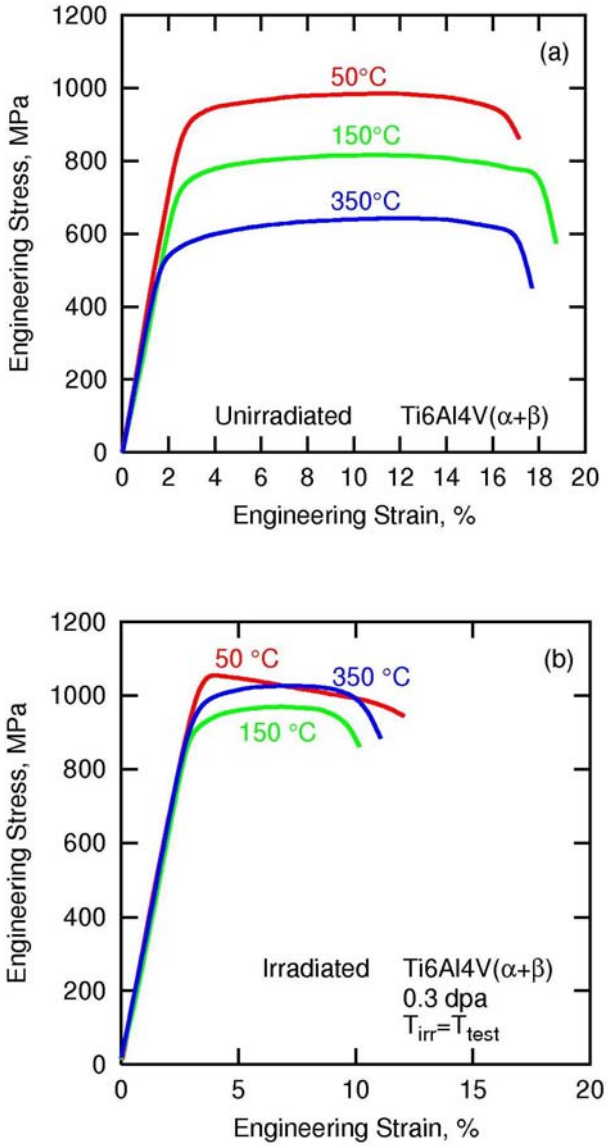

Figure 27. Stress-strain curves for (α + β) Ti-alloy tested at 50, 150 and 350°C in the (a) unirradiated and (b) irradiated (0.3 dpa at 50, 150 and 350°C) conditions. All tests were carried out in vacuum.

[3] TW3 – TVM - TICRFA

[4] S. Tähtinen, P. Moilanen, B.N. Singh and D.J. Edwards, J. Nucl. Mater. 307 – 311 (2002) 416.

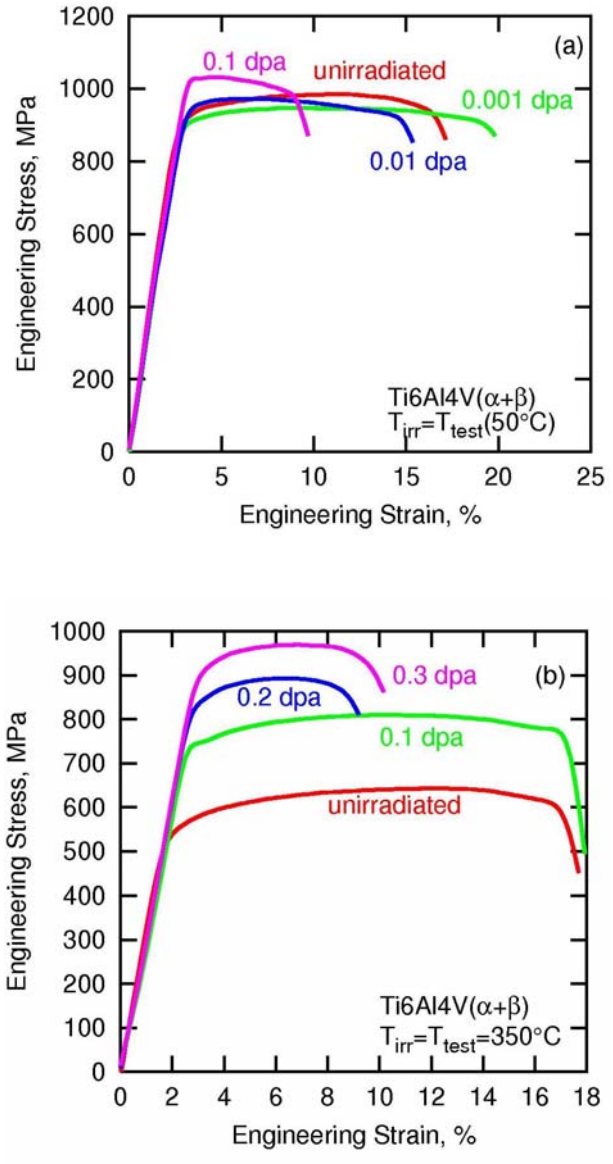

Figure 28. Stress-strain curves for (α + β) Ti-alloy tested in the unirradiated and irradiated (to different dose levels) at (a) 50°C and (b) 350°C. Tensile tests were carried out in vacuum and at the irradiation temperatures.

Some tensile specimens of the (α + β) Ti-alloy were irradiated at 150 °C to a dose level of ~0.3 dpa in a fission reactor in Hungary and at 50, 200 and 350 °C in the BR-2 reactor at Mol (Belgium). At 50°C, specimens were irradiated to dose levels of 10^{-3}, 10^{-2} and 10^{-1} dpa and at 350 °C to doses of 0.1, 0.2 and 0.3 dpa. Both unirradiated and irradiated specimens were tensile tested at the irradiation temperatures. All tests at 150 and 350 °C were carried out in vacuum. All tensile tests were performed using a strain rate of 1.3×10^{-3} s^{-1}.

The stress-strain curves for the (α + β) Ti-alloy tested at different temperatures both in the unirradiated and irradiated conditions are shown in Figure 27a and Figure 27b, respectively. The results show that the irradiation causes significant changes in the temperature dependence of the deformation behaviour. These changes cannot be rationalized in terms of the conventional irradiation hardening due to defect clusters but rather suggest that these changes may be due to irradiation induced precipitation and/or phase transformation.

Figure 28 shows the stress-strain curves illustrating the dose dependence of irradiation-induced hardening at (a) 50°C and (b) 350°C. The dose dependence of hardening at 50°C

showing first a decrease at very low doses and then an increase at higher doses (Figure 28a) also suggest some specific irradiation effects on the basic microstructural composition of the alloy other than the effect of irradiation induced defect microstructure. The irradiation at 350°C, on the other hand, exhibits a kind of a conventional increase in the hardening with increasing dose levels (Figure 28b) which may be attributed to the hardening due to irradiation-induced defects and their clusters.

3.3 Long-term technology

3.3.1 Effect of helium implantation and neutron irradiation on cavity formation in iron and Eurofer-97[5]

M. Eldrup, E. Johnson (*University of Copenhagen), B. N. Singh and P. Jung** (**Forschungszentrum Jülich, Association EURATOM-FZJ, Germany)*

As a part of the investigations of neutron irradiation effects in iron and low activation steels, Positron Annihilation Spectroscopy (PAS) and TEM investigations have been carried out to determine the effect of helium implantation and neutron irradiation on cavity formation in pure iron and Eurofer-97. The work has been a systematic continuation and expansion of the previous studies of these effects and has included He implanted and/or neutron irradiated pure Fe at 50 °C and 350 °C and Eurofer-97 at 350 °C. It has also comprised new He implanted Fe and Eurofer-97 specimens for tests of the reproducibility of results which have been reported previously. Generally the observed effects of He implantation and/or neutron irradiation are appreciably larger in Fe than in Eurofer-97 for both irradiation temperatures. Figure 29 illustrates the effects for Eurofer-97 by showing the changes with total displacement dose (implantation with 1, 10 and 100 appm He leads to displacement damage doses of 1.5×10^{-4}, 1.5×10^{-3}, and 1.5×10^{-2} dpa, respectively) of the mean positron lifetime for He implantation, neutron irradiation and neutron irradiation after He pre-implantation. As the figure shows, changes in the mean lifetime fall in the range up to 100 ps for Eurofer-97, while for Fe the range of mean lifetime variations is above 200 ps in the investigated dose range. This shows that the swelling in Eurofer-97 is smaller than in Fe. Figure 29 demonstrates that the effect of only He implantation is small at both implantation temperatures while the neutron irradiation effect is strong at 50 °C, but marginal at 350 °C. Pre-implantation of He has only a minor effect at 50 °C, while at 350 °C it strongly enhances the effect of neutron irradiation.

All the specimens, for which results are presented in Figure 29 and in previous reports, were He implanted with a dose rate of 0.02 appm He/s. In order to investigate the role of He implantation rate, experiments have been initiated with dose rates, which are 10 – 30 times lower.

[5] TW3 – TTMS - 007

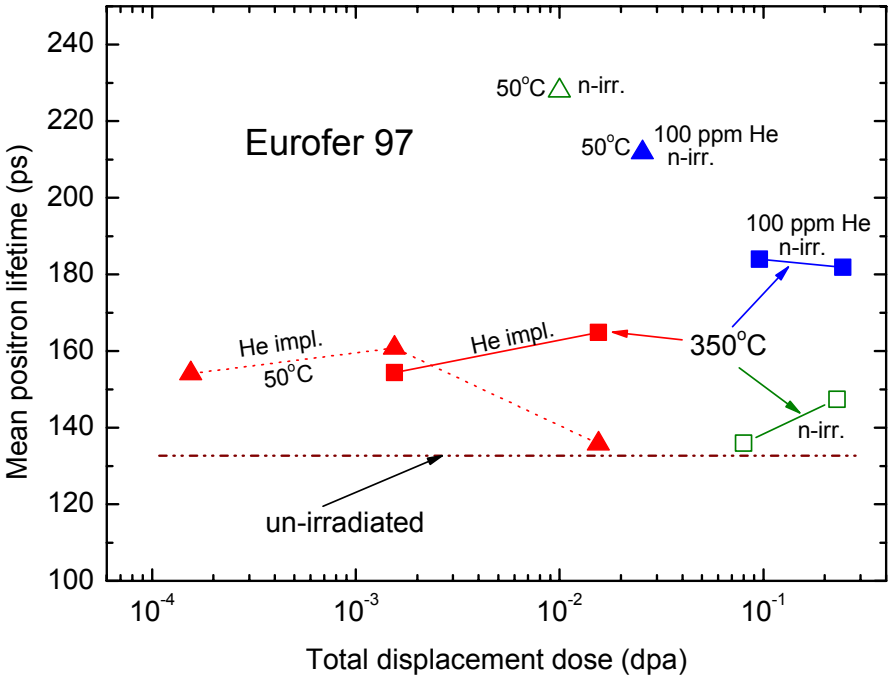

Figure 29. Mean positron lifetimes are shown as functions of total displacement dose for Eurofer-97 after He implantation, neutron irradiation or neutron irradiation with He pre-implanted.

Transmission Electron Microscopy examinations were carried out of pure Fe specimens, which were neutron irradiated at 350°C to doses of 0.08 dpa and 0.23 dpa. Examples of both cavity and loop microstructures are shown in Figure 30 and Figure 31, respectively. The micrographs show the presence of modest densities of resolvable loops and dislocations and a high density (~ 1.5×10^{21} m^{-3}) of voids with average sizes of about 2.5 nm and 4.0 nm, respectively. Transmission electron micrographs for the same specimens as used in Figure 31 but from different areas at (a) 0.08 dpa and (b) 0.23 dpa showing indication of dislocation decoration both at 0.08 and 0.23 dpa and of the formation of rafts of loops at 0.23 dpa are presented in Figure 32.

3.3.2 Influence of impurities on dislocation decoration and raft formation during neutron irradiation of bcc iron [6]

Ming Wen, N.M. Ghoniem* (*University of California Los Angeles, Los Angeles, USA) and B.N. Singh*

It is expected that the presence of impurity atoms may modify the microstructural evolution during irradiation because of elastic interaction between the impurity atoms and the clusters of self-interstitial atoms (SIAs) produced in the cascades. The interaction may cause, for example, reductions in 1-D diffusion coefficient of the SIA clusters and may modify the frequency of directional changes during 1-D transport of the SIA clusters. Consequently, the diffusion reaction kinetics may change between 1-D and 3-D limiting cases. Efforts are being made to understand the effect of such changes on damage accumulation behaviour.

[6] TW3 – TTMS - 007

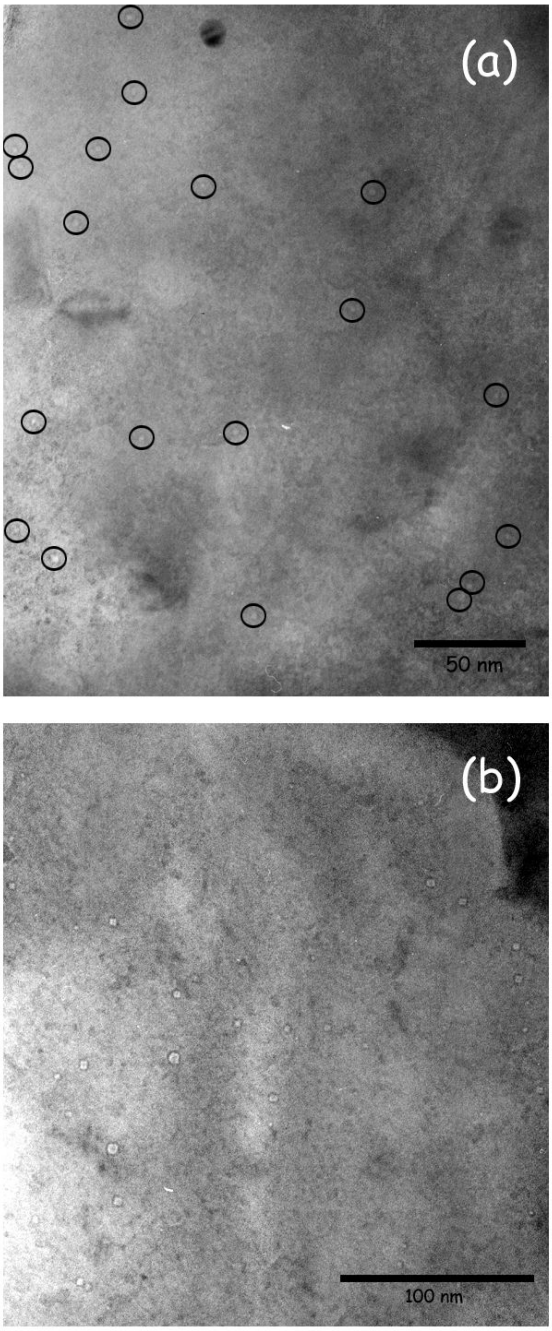

Figure 30. Transmission electron micrographs showing voids in pure Fe neutron irradiated at 350°C to a dose of (a) 0.08 dpa giving an average void size of ~ 2.5 nm and (b) 0.23 dpa giving an average void size of ~ 4.0 nm. In both cases the void density is about 1.5×10^{21} m^{-3}.

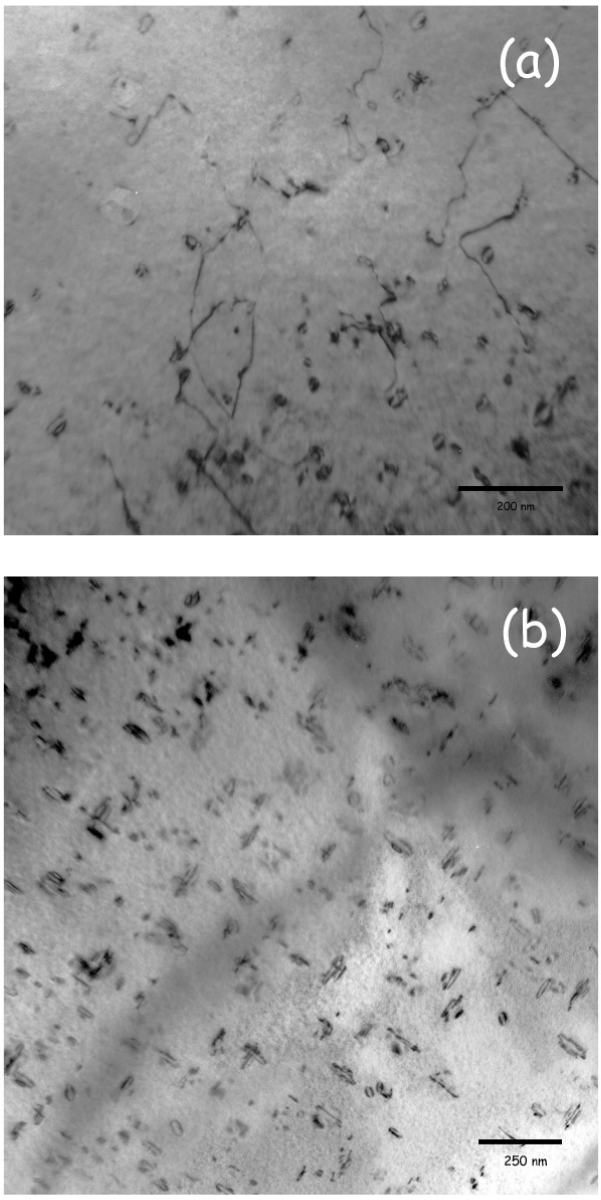

Figure 31. Transmission electron micrographs showing resolvable loops and dislocations in pure Fe neutron irradiated at 350°C to a dose of (a) 0.08 dpa and (b) 0.23 dpa.

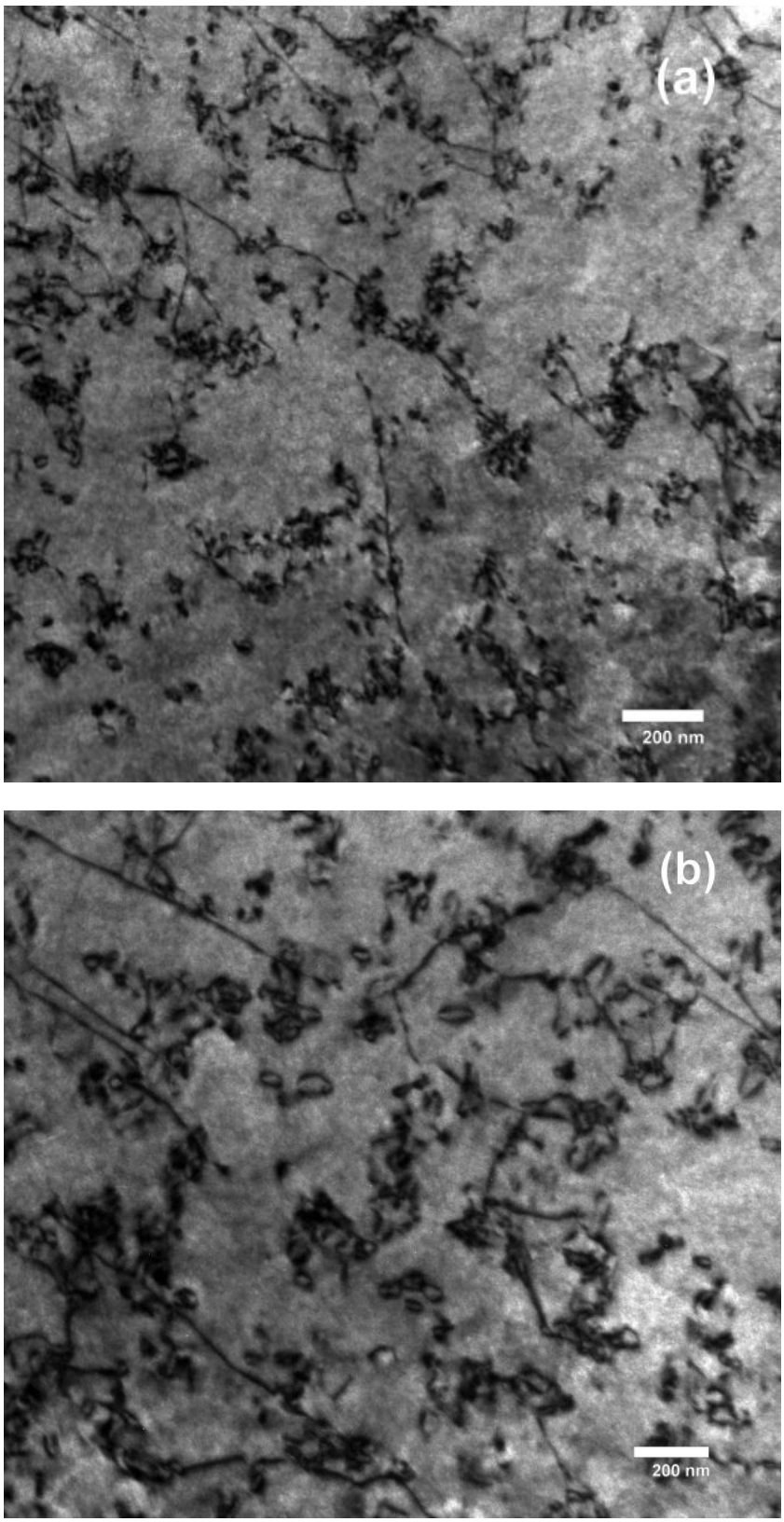

Figure 32. Transmission electron micrographs showing tendency for (a) dislocation decoration at 0.08 dpa and (b) formation of rafts of loops at 0.23 dpa in pure iron (i.e. without helium) irradiated at 350 ^{o}C.

It is well established theoretically that the 1-D diffusion of SIA clusters is necessary for the decoraton of dislocations with SIA clusters and the formation of rafts of SIA loops[7]. It has been also demonstrated experimentally that the presence of impurity atoms and alloying elements have strong effects on these processes[8]. It is of interest, therefore, to study the impact of impurity atoms in pure iron on damage accumulation and segregation of SIA clusters in the from of dislocation decoration and formation of rafts of SIA loops. A new Kinetic Monte Carlo (KMC) model has been used in the present work. In the present KMC simulations, the defects generated by 40 keV cascades corresponding to a damage rate of 5 x 10^{-8} dpa/s are introduced at appropriate frequency in the simulation box of 350a x 350a x 350a, where a is the lattice parameter. The point defect production statistics, the magnitude of 1-D glide of SIA clusters and the frequency of change in the direction of defusion of these clusters are taken from the results of MD simulations reported for iron. In the present KMC model the elastic interaction between various components of the microstructure including SIA clusters and dislocations is explicitly incorporated. The influence of impurities is included as additional sources of internal strains. The substitutional impurities are treated as spherical dilatation centres randomly distributed at lattice sites. The infinitesimal prismatic dislocation loop approximation and the size dependent 1-D diffusional behaviour of SIA clusters are used. The KMC simulations are carried out for impurity concentration of 100 appm at irradiation temperature of 300 K.

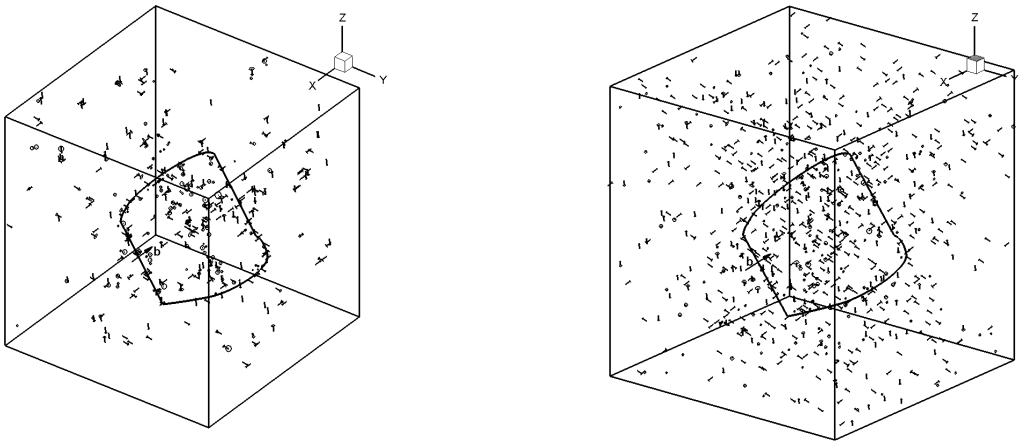

Figure 33. Spatial distribution of SIA clusters in bcc Fe irradiated at 300 K to a dose level of 7.1×10^{-4} dpa, (a) without impurity (b) with randomly distributed 100 appm of impurity atoms.

The presence of impurities affects the motion of 1-D diffusing SIA clusters substantially and the mean free path for 1-D motion of the cluster is reduced significantly. Furthermore, the clusters get trapped in the vicinity of impurities. Because of these reductions, the frequency of interactions between these SIA clusters and the extended dislocation line is likely to be reduced. The cluster-cluster interaction on the other hand is likely to be enhanced. The net result would be that in the presence of impurity atoms the density of homogeneously distributed SIA clusters would increase and the processes of dislocation decoration and raft formation would be slowed down. Figure 33 shows examples of the results of KMC simulations in pure bcc iron (Figure 33a) and iron containing 100 appm of substitutional

[7] H. Trinkaus, B.N. Singh and A.J.E. Foreman, J. Nucl. Mater. 249 (1997) 91.

[8] B.N. Singh, J.H. Evans, A. Horsewell, P. Toft and G.V. Müller, J. Nucl. Mater. 258 – 263 (1998) 865.

impurity (Figure 33b). The simulations refer to a dose level of 7.1 x 10^{-4} dpa at 300 K. Figure 33a shows that in the case of pure iron the decoration of the dislocation with SIA clusters begin to occur already at a dose level of 7.1 x 10^{-4} dpa. However, in the case of iron containing 100 appm of impurity, there is no indication of any decoration of dislocation or the formation of rafts of SIA clusters at this dose level. Besides, the density of the accumulated SIA clusters in the iron containing impurity is a factor of two higher than in the case of pure iron (Figure 33a).

3.3.3 Cavity evolution in bcc iron during neutron irradiation with and without helium implantation[9]

S.I. Golubov (*Oak Ridge National Laboratory, Oak Ridge, USA), B.N. Singh and M. Eldrup*

To our knowledge, there exists no theoretical framework at present within which the details of cavity nucleation can be adequately treated particularly for the condition of concurrent generation of cascades and helium atoms. It is well known, however, that the creation of an excess of vacancies (i.e. vacancy supersaturation) during irradiation and the concentration of the available gas atoms are two most potent parameters that control the scale of cavity nucleation at a given irradiation temperature.

The present work was initiated to perform detailed numerical calculations of temporal evolution of vacancy concentration and supersaturation and kinetics of cavity nucleation and growth under cascade damage conditions. The computer code developed earlier to treat the problem of void swelling within the framework of the production bias model (PBM) has been modified to include the treatment of concurrent generation of helium and displacement cascades. In order to investigate the effect of helium on the evolution of cavity microstructure under cascade damage condition, it was necessary to find the solution of two-dimensional kinetic equation for the size distribution function of helium-vacancy clusters in pure iron implanted with helium or irradiated with neutrons. In order to reduce the number of equations needed to be solved for describing the evolution of helium-vacancy complexes, a new grouping method has been employed to integrate the kinetic equations.

While calculating the impact of helium atoms on cavity nucleation particularly under the conditions of concurrent production of displacement cascades and mutational helium atoms two further complications arise. The first problem arises from the fact that the diffusion mechanism of helium atoms under these conditions still remains uncertain. On the other hand, the diffusivity of helium plays a vital role in determining the scale of cavity nucleation. The second problem arises from the fact that small cavities may perform Brownian-like motion. The coalescence of these small, mobile cavities may reduce the final density of cavities. For these reasons computer code for the numerical calculation of cavity density during helium implantation as well as during neutron irradiation after helium implantation was revised.

The revised code makes it possible to calculate the cavity nucleation using different mechanisms for helium diffusion and to evaluate the role of Brownian-like motion and coalescence of embryonic cavities on the final cavity density. In the present calculations we have considered the diffusion of helium via the so-called “replacement mechanism” or via “di-vacancy mechanism”. The Brownian-like motion is assumed to occur via the surface diffusion controlled mechanism. Under all these conditions, the evolution of vacancy supersaturation is calculated within the framework of the PBM. With these provisions we have first calculated the size distribution after neutron irradiation (Figure 34a) and after helium implantation at 50^{o}C (Figure 34b).

[9] TW3 – TTMS - 007

Figure 34a shows size distributions of cavities at different dose level between 10^{-3} – 0.7 dpa calculated for the irradiation temperature of 50°C. The surviving defect fraction (1 - ε_r) is taken to be 20% and the fraction of glissile SIA clusters is taken to be 25%. The dislocation density is taken to be 10^{13} m^{-2}. The mean cavity diameter at the dose level of 0.7 dpa is about 1 nm which is in good agreement with the experimental results for pure iron neutron irradiated at ~70°C to a dose level of 0.72 dpa[10].

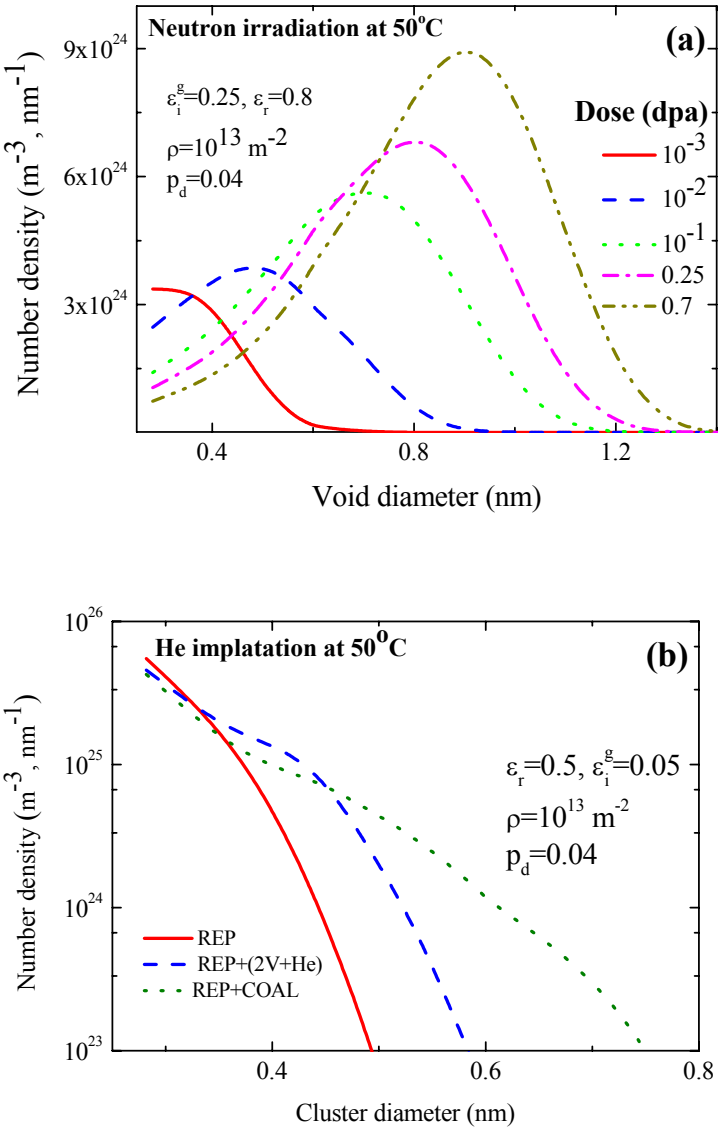

Figure 34. Size distribution functions of voids in neutron irradiated iron at 50°C (a) calculated in the framework of PBM to different doses for the case of no V-cluster mobility and He-V clusters in alpha particle irradiated iron at 50°C (b) calculated for different mechanisms of He transport: replacement mechanism, mobility of the (2V+He) clusters and coalescence of the clusters. Note that the mean diameter of voids at 0.25 dpa calculated is slightly larger than that estimated by PAS. However the mean diameter calculated at 0.7 dpa (about 1 nm) is close to that found in Ref. 10.

The size distributions of cavities in iron helium implanted at 50°C to a helium concentration level of 100 appm (corresponding to a displacement dose level of ~2 x 10^{-2} dpa) are shown in Figure 34b. The calculations are carried out for both diffusion mechanisms (i.e.

[10] M. Eldrup, B.N. Singh, S. Zinkle, T.S. Byun and K. Farrel, J. Nucl. Mater. 307 – 311 (2002) 912.

replacement and divacancy). The influence of Brownian-like motion and coalescence is also evaluated. The damage parameters (ε_r and ε_i^g) are taken to represent the lower recoil energy expected during helium implantation. It should be noted that the size distributions are considerably narrower than those in the case of neutron irradiation.

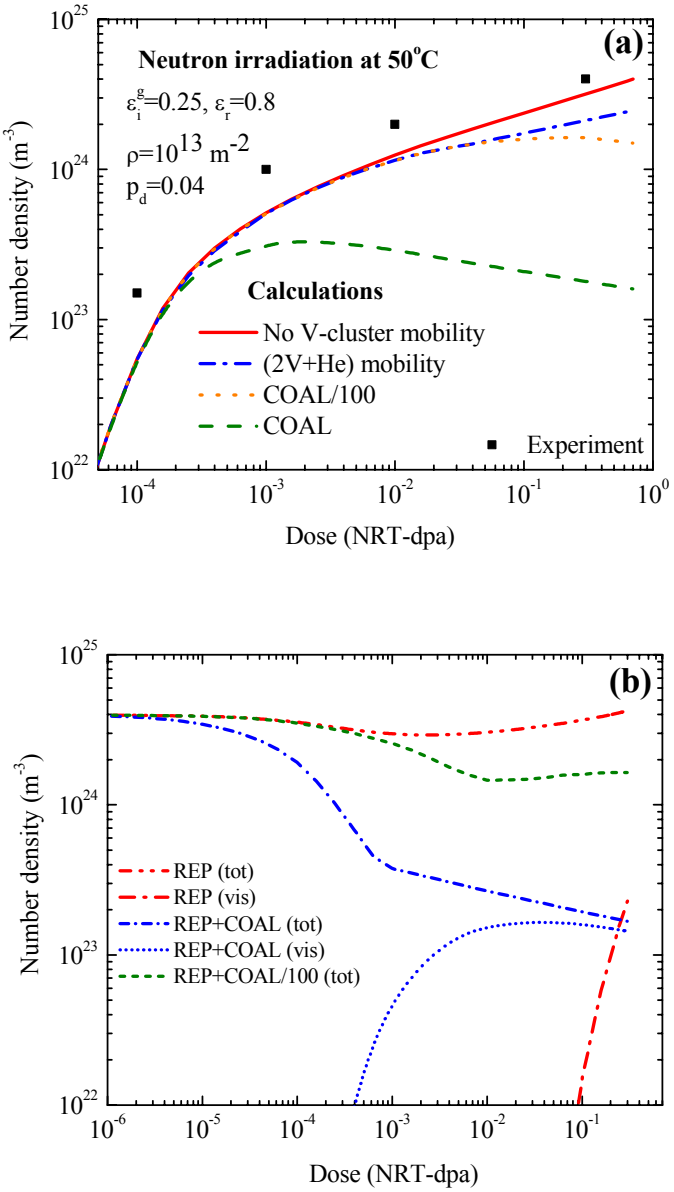

Figure 35. Dose dependence of the number density of voids in (a) neutron irradiated iron at 50°C and (b) the number density of He- V clusters in neutron irradiated iron at 50°C which was preimplanted with 100 appm He at 50°C.

Figure 35a shows the dose dependence of cavity density in iron neutron irradiated at 50°C calculated using two different diffusion mechanisms for helium. The influence of Brownian-like motion and coalescence is also shown. The dose dependence of nano-voids determined by the positron annihilation spectroscopy (PAS) technique[10] is also shown in the figure. The calculated results with no vacancy-cluster mobility are in reasonable agreement with the experimental results. It is also fairly clear that the Brownian-like motion and the resulting coalescence lead to cavity densities that are considerably lower than the experimental results. In other words, under these experimental conditions, the Brownian-like motion is significantly reduced. The dose dependence of cavity density in iron calculated for neutron irradiated at 50°C after helium implantation (100 appm) at 50°C is shown in Figure 35b.

3.4 Underlying technology

3.4.1 Impact of impurities on the diffusion reaction kinetics of interstitial cluters under cascade damage conditions

H. Trinkaus (*Forschungszentrum Jülich, Jülich, Germany), B.N. Singh and S.I. Golubov** (**Oak Ridge National Laboratory, Oak Ridge, USA)*

In metals exposed to cascade producing irradiation such as in a fusion environment, the damage accumulation at low doses (<1dpa) and at medium temperatures (between 0.2 and $0.4T_m$, T_m: melting temperature) occurs in a spatially highly heterogeneous and segregated fashion: self-interstitial atoms (SIAs) segregate in the form of dislocation loops near dislocations or form rafts of loops while vacancies accumulate in the form of voids in between and, intensified, near grain boundaries. These features depend on crystal structure and instantaneous microstructure as well as on the composition of the metal, in particular on the concentration of impurities which generally tend to blur these features.

During the last decade, these phenomena have been rationalized in terms of intra-cascade clustering of both vacancies and SIAs, and one-dimensional (1D) diffusion of SIA clusters. However, various features in damage accumulation, such as its tendency to change with increasing impurity concentration from highly heterogeneous towards more homogeneous and the stability of once formed void super-lattices at high doses, can not be understood unless the 1D diffusion of SIA clusters is assumed to be disturbed, for instance by changes between equivalent diffusion directions and/or diffusion transversal to the 1D direction, both resulting in diffusion reaction kinetics (RK) between the 1D and 3D limiting cases.

Generalizing our previous treatment[11] we have recently shown that the 1D to 3D RK of SIA clusters induced by 1D direction changes and transversal diffusion can be described by one analytical single-variable function ("master curve") interpolating between the 1D and 3D limiting cases[12] 12. The intrinsic parameters characterising this general RK of SIA clusters are the ratio of the transversal (2D) to longitudinal (1D) diffusion coefficient, $\delta = D_{tr}/D_{lo}$, and the mean 1D diffusion length covered during the time τ_{ch} between two direction changes, $l_{ch} = \sqrt{2D_{lo}\tau_{ch}}$.

---

[11] H. Trinkans, H. L. Heinisch, A. V. Barashov, S. I. Golubov, and B. N. Singh, Phys. Rev. B66, 060105 (R) (2002)

[12] H. Trinkans, B. N. Singh and S. I. Golubov, Proc. 2nd Int. Conf. on "Multiscale Materials Modelling, Oct. 11-15, 2004, Los Angeles, ed. N.M. Ghoniem, p. 561

In the presence of impurities, both controlling parameters, δ and l_{ch}, are affected by the elastic interaction of the SIA clusters (SIA-type dislocation loops) with the impurities, and this occurs mainly via a reduction of the 1D diffusion coefficient D_{lo} in a kind of nano-scale solution hardening, which changes the RK more towards 3D. An impurity atom in or close to the glide cylinder of a SIA cluster represents a row of barriers or (temporary) trapping sites depending on the sign of the volume misfit and the position of the impurity atom relative to the glide cylinder. Two different problems have to be solved: (1) the formal description of 1D diffusion (D_{lo}) in the presence of rows of barriers and trapping sites, and (2) the quantitative determination of the elastic interaction of loop-like SIA clusters with impurity atoms. Concerning (1), we have derived an approximate expression for D_{lo} for the case of low impurity concentration where a simultaneous significant interaction of two (or more) impurities with a certain SIA cluster is unlikely to occur. Concerning (2), we have estimated the loop-impurity interaction energy on the basis of elastic continuum theory which is, however, doubtful close to the core of a dislocation loop just where the interaction is strongest and thus most important. In view of these limitations, our results must be considered to be still preliminary.

On the basis of these approximations, we have estimated the impurity induced changes in D_{lo} and, via this, in l_{ch} and δ, as a function of the loop size, the relative volume misfit, e, and the concentration, c_i, of impurity atoms, and of the temperature. Figure 36a shows that impurities can significantly increase the transversal to longitudinal diffusion ratio, δ, thus decreasing the diffusion anisotropy (and by this the character of the RK), particularly at the lower temperature side. Because of the very fast undisturbed 1D diffusion, δ remains, however, small, even for the relatively high values $c_i = 1\%$ and $e = 0.2$ (assumed here).

The effect of impurities on the character of the RK of SIA clusters and the resulting damage accumulation can be discussed in terms of impurity-induced changes in the parameters δ and l_{ch} controlling the RK. We have illustrated this by analyzing the effect of impurities on a feature typical for 1D RK of SIAs: the saturation of void growth at high doses. For pure 1D RK, the void size (radius R) converges to a constant saturation size of the order of a few nm, $R_s^{1D} = \pi d$, determined solely by the diameter of the dislocations for the absorption of SIA clusters, d, independent of the sink densities. Any disturbance of the pure 1D RK such as the additional production of 3D diffusing single SIAs, 1D direction changes and transversal diffusion of SIA clusters results, however, in an increase of the saturation size R_s compared to that for pure 1D RK, depending on the sink densities, particularly when the disturbance is enhanced by impurities.

Figure 36b illustrates this dependence for transversal diffusion: R_s increases with decreasing void density, particularly in the presence of impurities. This may explain why in FCC metals under neutron irradiation where, on the one hand, transmutation elements representing impurities are continuously produced, and, on the other hand, compared to BCC, only relatively low void densities are formed, generally no void growth saturation is observed.

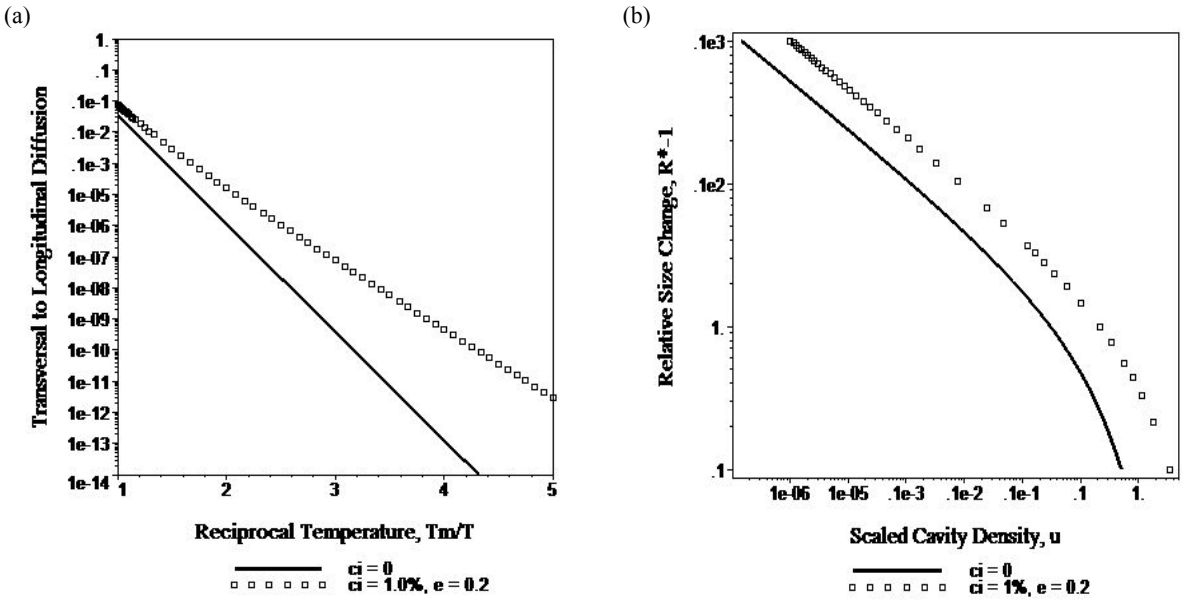

Figure 36. Illustration of the effect of impurities: (a) Diffusion ratio, $\delta = D_{tr}/ D_{lo}$, vs reciprocal homologous temperature, T_m/T, and (b) relative change of saturated void size, $R^* - 1 = R_s/(\pi d) - 1$, vs scaled void density, $u = (\pi d)^3 N/\sqrt{\delta_0}$ at 0.4 T_m assuming void sink dominance, for pure a metal ($c_i = 0$, $\delta = \delta_0$) and a metal containing c_i = 1% impurity atoms with relative volume misfit $e = 0.2$.

3.4.2 Reaction kinetics for defect diffusion by preferential one-dimensional migration

Howard L. Heinisch (*Pacific Northwest National Laboratory, Richland, WA, USA), Helmut Trinkaus** (**Forschungszentrum Jülich, Jülich, Germany) and B.N. Singh*

The diffusion reaction kinetics of mobile components in crystalline solids are highly dependent on the dimension of their diffusion processes. For example, clusters of interstitial crowdion defects in irradiated metals readily take the form of small dislocation loops that can migrate with very low activation energy by gliding in a one-dimensional (1D) random walk along one of the close-packed directions of the crystal. Such loops can occasionally be induced by thermally activated processes or defect interactions to change the direction of their glide and continue gliding one-dimensionally along a different close-packed direction. Thus, they undergo three-dimensional (3D) diffusion through the crystal along a series of different 1D migration paths. The sink strengths for the absorption of these loops into microstructural features depends not only on the nature of the field of absorbers and the characteristics of their interactions with the loops, but also on the frequency of direction changes of the loops. The sink strengths can vary by orders of magnitude over the range of possible direction-change frequencies from essentially pure 1D migration (no direction changes) to pure 3D migration (a possible direction change for every defect "hop"). The relationship between sink-strength and frequency of direction change for "1D/3D" migrating defects has been studied in detail in previous work[11], where an analytical description over the entire range from pure 1D to pure 3D precisely describes the results of kinetic Monte Carlo computer simulations.

Another potential migration mechanism, especially for larger glissile loops of this type, is conservative climb, whereby the loop migrates transverse to its glide direction by diffusion of point defects along the perimeter of the loop. This results in 2D migration of the loop in the

plane of the loop. "Preferential-1D migration" occurs when a loop glides in 1D, but makes an occasional 2D transverse climb excursion, followed by continuing glide along the original 1D direction. The variation of sink strength as a function of the frequency of transverse migration events for defects undergoing preferential-1D migration is a topic under current study, both analytically and by computer simulations.

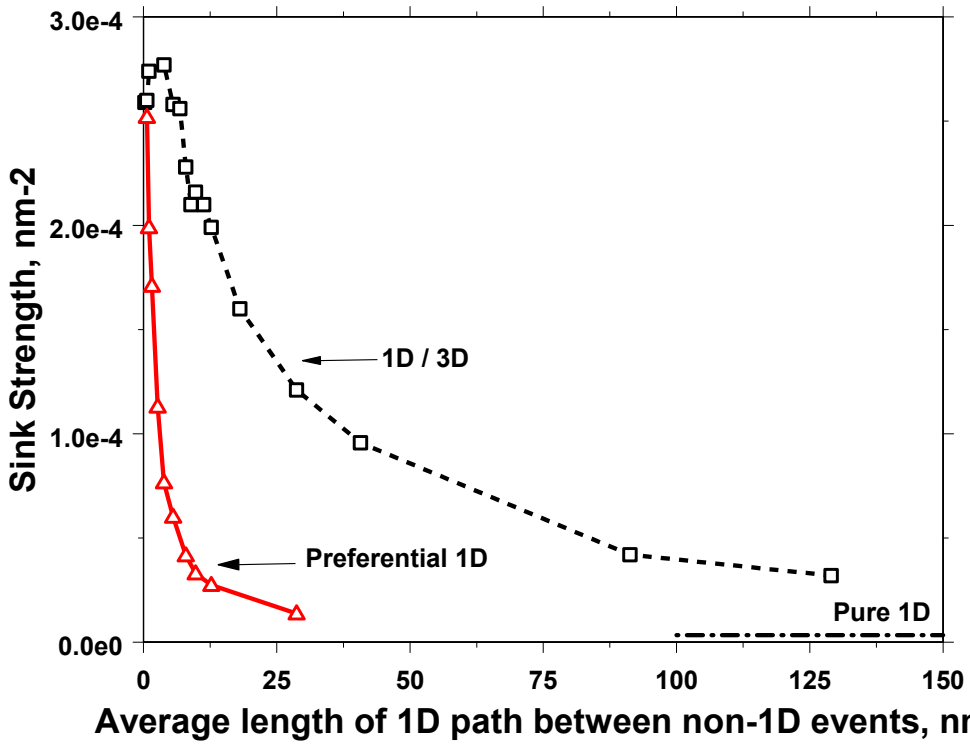

Figure 37. A comparison of sink strengths for defects diffusing by preferential 1D and by1D-3D migration as a function of the average length of the 1D path between non-1D events (linear scale).

Preliminary results of recent computer simulations are shown in Figure 37, where the sink strengths for preferential-1D migration are compared with those for 1D/3D migration for the same set of mobile loops and stationary absorbers. Sink strengths are plotted as a function of the average 1D path length between non-1D migration events. The results are presented in terms of sink strength as a function of the distance between interruptions of the 1D motion. Thus, for the reference 1D/3D case, the "interruptions of 1D" are the changes of direction of the 1D glide, while for the preferential-1D data, the "interruptions" are the transverse 2D climb hops. An important difference between these two diffusion modes, of course, is that in the 1D/3D migration the direction of the 1D migration changes at each interruption, while for the preferential case, the defect always resumes 1D glide migration along the same crystallographic direction after each climb excursion. The results in both cases are for the same simulation geometry, i.e., the same cubic volume containing the same distribution of spherical absorbers of uniform radius (R=30 half lattice parameters or 5.4 nm in Cu). Each data point on the graph is the average for 1000 migrating defects starting at random locations. The lines simply connect the data points.

Analytical expressions have been derived to describe the transition from 1-D to 3-D for preferential-1D, and further studies of more complex combinations of climb, glide and direction change of migrating defects are under consideration.

3.4.3 Positron annihilation spectroscopy investigations of CuCrZr alloy with different heat treatments

Peter Domonkos (*Department of Nuclear Physics and Technology, Slovak University of Technology, Bratislava, Slovak Republic), Morten Eldrup and B.N. Singh*

The characterization of precipitate formed as a consequence of applied heat treatment (HT) and observed by Transmission Electron Microscopy (TEM) was the main objective to perform the study of the CuCrZr (Outokumpu) structure using Positron Annihilation Spectroscopy (PAS). We have therefore measured and evaluated the PAS lifetime spectra of the heat treated CuCrZr samples using the same heat treatment conditions (Table1) as reported earlier[13]. In agreement with the results obtained by TEM we have observed a strong influence of the heat treatment on the PAS results.

Table 1**.** Summary of the heat treatments for CuCrZr (Outokumpu) alloy.

Heat treatment (HT)	**Description of applied HT**
SA	Solution annealing (SA) at 960°C for 3 h followed by water quench (WQ)
PA	Prime ageing (PA): SA + ageing at 460°C for 3 h followed by WQ
PA+HT1	PA + ageing at 600°C for 1 h + WQ
PA+HT2	PA + ageing at 600°C for 4 h + WQ
PA+HT3	PA+ ageing at 700°C for 4 h + WQ
PA+HT4	PA+ ageing at 850°C for 4 h + WQ
PA+HT5	PA+HT4+960°C for 3 h + WQ

A conventional two-detector positron lifetime system was used for the measurements. In total, 69 positron lifetime measurements were performed (46 on CuCrZr and 23 on reference Cu sample), with more than 3.5×10^6 events in each measured spectrum. For each of the 7 heat treatments (Table 1) measurements were performed several times on each sample set as well as on different sets in order to estimate the scatter of the results. All the measurements were performed at room temperature (RT).

The measured PAS lifetime spectra could be decomposed into two components, with lifetimes τ_1 and τ_2 and corresponding intensities I_1 and I_2 ($I_1+I_2=100\%$), shown in Figure 38 and Figure 39, respectively. As seen in Figure 38, in non-irradiated CuCrZr alloy a well defined long lifetime τ_2 was observed, which was basically constant over the whole range of HT (176±8ps), except for the SA and PA+HT5 states, where τ_2 is slightly higher (200±15ps). The measured long lifetime τ_2 is probably associated with the vacancy-type defects at the precipitate matrix interface, believed to arise from lattice mismatch between matrix and precipitates. In contrast to the modest variation of the defect lifetime, its intensity I_2 exhibits a strong variation with heat treatment (Figure 39). By application of a simple so-called trapping

[13] B. N. Singh, D. J. Edwards and P. Toft, Risø-Report: Risø-R-1345(EN), June 2002.

model it is possible to estimate from the data in Figure 38 and Figure 39 the average density of the defects that act as positron traps. The numbers come out between $C_{vac}=1.3\times10^{23}$ m^{-3} (SA) and $C_{vac}=2.3\times10^{24}$ m^{-3} (PA+HT1) assuming the trapping sites to be vacancy-like.

The PAS measurements, performed at non-irradiated materials, will be used as a starting point for subsequent investigations of neutron irradiated CuCrZr alloys.

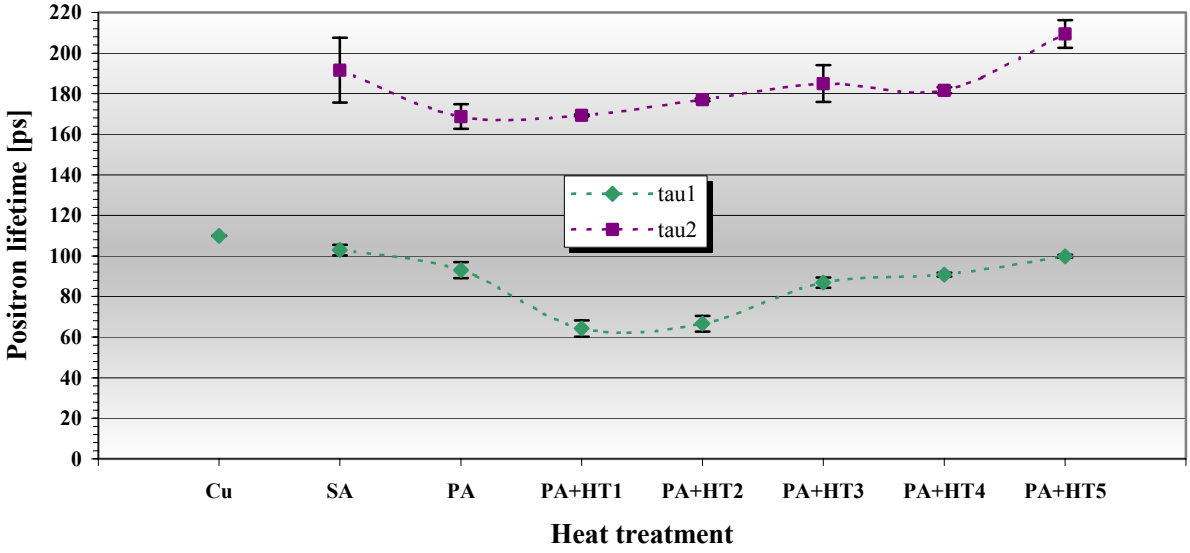

Figure 38. The HT effect investigated by PAS measurements for non-irradiated CuCrZr alloy samples (Table 1). The positron lifetime components: τ_1 – shortest lifetime, τ_2 – long defect lifetime. The lifetime value for pure Cu is 110 ps, as indicated in the figure.

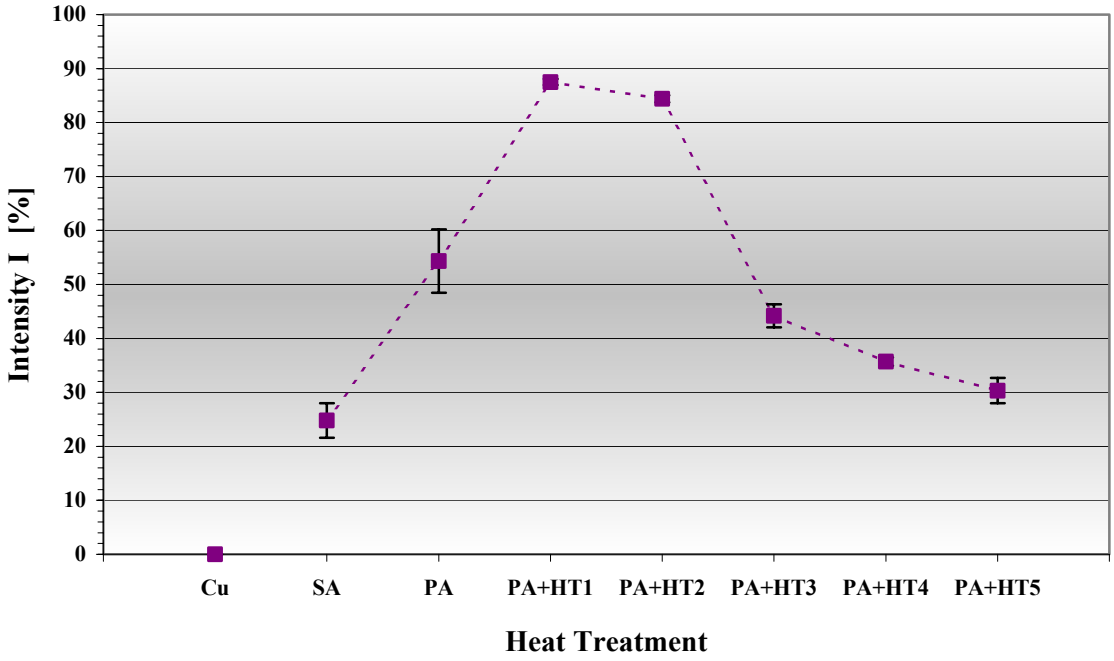

Figure 39. The intensity I_2 of the long-lived component (due to positrons trapped in defects) in PAS spectra for non-irradiated CuCrZr alloy for various heat treatments (Table 1).

3.5 Publications and conference proceedings

3.5.1 International publications

Edwards, D.J.; Singh, B.N., Evolution of cleared channels in neutron-irradiated pure copper as a function of tensile strain. 11. International Conference on Fusion Reactor Materials (ICFRM-11), Kyoto (JP), 7-12 Dec 2003. J. Nucl. Mater. (2004) v. 329-333 p. 1072-1077

Edwards, D.J.; Singh, B.N., Evolution of cleared channels in neutron-irradiated pure copper as a function of tensile strain. In: Fusion materials. Semiannual progress report for the period ending December 31, 2003. DOE/ER-0313/35 (2004) p. 136-138

Eldrup, M.; Singh, B.N.; Edwards, D.J.; Nagai, Y.; Ohkubo, H.; Hasegawa, M., Neutron irradiated copper: Is the main positron lifetime component due to stacking fault tetrahedra?. 13. International conference on positron annihilation - ICPA-13, Kyoto (JP), 7-12 Sep 2003. Mater. Sci. Forum (2004) v. 445-446 p. 21-24

Li, M.; Singh, B.N.; Stubbins, J.F., Room temperature creep-fatigue response of selected copper alloys for high heat flux applications. 11. International Conference on Fusion Reactor Materials (ICFRM-11), Kyoto (JP), 7-12 Dec 2003. J. Nucl. Mater. (2004) v. 329-333 p. 865-869

Peacock, A.T.; Barabash, V.; Dänner, W.; Rödig, M.; Lorenzetto, P.; Marmy, P.; Merola, M.; Singh, B.N.; Tähtinen, S.; van der Laan, J.; Wu, C.H., Overview of recent European materials R and D activities related to ITER. 11. International Conference on Fusion Reactor Materials (ICFRM-11), Kyoto (JP), 7-12 Dec 2003. J. Nucl. Mater. (2004) v. 329-333 p. 173-177

Singh, B.N.; Golubov, S.I.; Trinkaus, H.; Edwards, D.J.; Eldrup, M., Review. Evolution of stacking fault tetrahedra and its role in defect accumulation under cascade damage conditions. J. Nucl. Mater. (2004) v. 328 p. 77-87

Thorsen, P.A.; Bilde-Sørensen, J.B.; Singh, B.N., Bubble formation at grain boundaries in helium implanted copper. Scr. Mater. (2004) v. 51 p. 557-560

Wen, M.; Ghoniem, N. M.; Singh, B.N., Kinetic Monte Carlo simulations of dislocation decoration and raft formation in bcc-iron under cascade irradiation. In: Fusion materials. Semiannual progress report for the period ending December 31, 2003. DOE/ER-0313/35 (2004) p. 201-208

3.5.2 Danish reports

Bindslev, H.; Singh, B.N (eds.), Association Euratom - Risø National Laboratory annual progress report 2003. Risø-R-1468(EN) (2004) 60 p.

Singh, B.N; Edwards, D.J.; Tähtinen, S., Effect of heat treatments on precipitate microstructure and mechanical properties of CuCrZr alloy. Risø-R-1436(EN) (2004) 24 p.

Singh, B.N; Edwards, D.J.; Bilde-Sørensen, J.B., Initiation and propagation of cleared channels in neutron-irradiated pure copper and a precipitation hardened CuCrZr alloy. Risø-R-1485(EN) (2004) 18 p.

Singh, B.N; Edwards, D.J.; Tähtinen, S.; Moilanen, P.; Jacquet, P.; Dekeyser, J., Final report on in-reactor tensile tests on OFHC - Copper and CuCrZr alloy. Risø-R-1481(EN) (2004) 47 p.

3.5.3 International reports

Moilanen, P.; Tähtinen, S.; Singh, B.N.; Jacquet, P., TW2-TVV-SITU, In-situ investigation of the mechanical performance and life time of copper. BTUO 76-031127 (2004) 24 p.

Tähtinen, S.; Singh, B.N., Effect of heat treatment and neutron irradiation on tensile and fracture toughness properties of CuCrZr/316L(N) HIP joints. BTUO 73-041299 (2004) 14 p.

3.5.4 Published conference contributions

Golubov, S.I.; Singh, B.N.; Eldrup, M.; Ovcharenko, A.M.; Stoller, R.E., Investigations of cavity evolution in bcc iron implanted with helium and subsequently irradiated with neutrons. In: Conference proceedings. 2. International conference on multiscale materials modeling (MMM-2), Los Angeles, CA (US), 11-15 Oct 2004. Ghoniem, N.M. (ed.), (University of California, Los Angeles, 2004) p. 501-503

Trinkaus, H.; Singh, B.N.; Golubov, S.I., Reaction kinetics of SIA clusters and damage accumulation in metals under cascade irradiation: Impact of impurities. In: Conference proceedings. 2. International conference on multiscale materials modeling (MMM-2), Los Angeles, CA (US), 11-15 Oct 2004. Ghoniem, N.M. (ed.), (University of California, Los Angeles, 2004) p. 561-563

Wen, M.; Ghoniem, N.M.; Singh, B.N., The influence of impurities and alloying on dislocation decoration and raft formation during neutron irradiation of bcc metals. In: Conference proceedings. 2. International conference on multiscale materials modeling (MMM-2), Los Angeles, CA (US), 11-15 Oct 2004. Ghoniem, N.M. (ed.), (University of California, Los Angeles, 2004) p. 567-569

3.5.5 Unpublished international conference contributions

Edwards, D.J.; Singh, B.N., Cleared channel formation in irradiated metals. Workshop on fundamental aspects of radiation damage, Lake Arrowhead (US), 16-18 Oct 2004. Unpublished.

Eldrup, M.; Singh, B.N.; Edwards, D.J.; Nagai, Y.; Ohkubo, H.; Hasegawa, M., Defects in neutron irradiated copper investigated by positron annihilation spectroscopy. 35. Polish seminar on positron annihilation, Turawa (PL), 19-24 Sep 2004. Unpublished.

Heinisch, H.L.; Singh, B.N.; Trinkaus, H., KMC studies of the reaction kinetics of defects that diffuse one-dimensionally with occasional transverse migration. In: Conference proceedings. 2. International conference on multiscale materials modeling (MMM-2), Los Angeles, CA (US), 11-15 Oct 2004. Ghoniem, N.M. (ed.), (University of California, Los Angeles, 2004) p. 507

Singh, B.N., In-reactor deformation behaviour. Workshop on fundamental aspects of radiation damage, Lake Arrowhead (US), 16-18 Oct 2004. Unpublished.

Trinkaus, H.; Singh, B.N.; Golubov, S.I., Some aspects of defect accumulation in copper under cascade damage conditions at low temperatures. Workshop on fundamental aspects of radiation damage, Lake Arrowhead (US), 16-18 Oct 2004. Unpublished.

Tähtinen, S.; Singh, B.N.; Moilanen, P.; Jacquet, P.; Dekeyser, J.; Edwards, D.J., Deformation behaviour of copper under in-reactor uniaxial tensile tests (poster). 23. Symposium on fusion technology (SOFT), Venice (IT), 20-24 Sep 2004. Unpublished.

Title and authors

Association Euratom – Risø National Laboratory
Annual Progress Report 2004

Edited by H. Bindslev and B.N. Singh

ISBN	ISSN
87-550-3449-7	0106-2840; 1396-3449

Department or group	Date
Optics and Plasma Research Department	June 2005

Pages	Tables	Illustrations	References
61	1	39	24

Abstract (max. 2000 characters)

Abstract The programme of the Research Unit of the Fusion Association Euratom - Risø National Laboratory covers work in fusion plasma physics and in fusion technology. The fusion plasma physics research focuses on turbulence and transport, and its interaction with the plasma equilibrium and particles. The effort includes both first principles based modelling, and experimental observations of turbulence and of fast ion dynamics by collective Thomson scattering. The activities in technology cover investigations of radiation damage of fusion reactor materials. These activities contribute to the Next Step, the Long-term and the Underlying Fusion Technology programme. A summary is presented of the results obtained in the Research Unit during 2004.

Descriptors INIS/EDB

CHARGED-PARTICLE TRANSPORT; ENERGY TRANSFER; MAGNETIC CONFINEMENT; NONLINEAR PROBLEMS; PHYSICAL RADIATION EFFECTS; PLASMA DIAGNOSTICS; PLASMA SIMULATION; PROGRESS REPORT; RISOE NATIONAL LABORATORY; THERMONUCLEAR REACTIONS; THERMONUCLEAR REACTOR MATERIALS; THOMSON SCATTERING; TOKAMAK DEVICES; TURBULENCE